Controlled Foaming on Cereal Protein
Rheological Properties of a Model System for Solid Foams
ALBERTO LIPIA
Department of Materials and Manufacturing Technology
Chalmers University of Technology

ABSTRACT

Foamed materials are used today in many applications such as packaging, insulation, protection, construction materials and in food as well.

What differentiates them, in addition to the physical and chemical properties of the materials, is their cell structure giving different foam properties, like porosity, density, strength and texture. Thus, keeping the foaming process under control is fundamental. It can yield to different products, characterized by their own structure, but made up with the same materials.

In this project a model foam system of a cereal prolamin protein, starch, plasticizer and foaming agents, with applications in gluten free food and insulation foams, was developed and characterized.

The protein zein was mixed with maize starch, plasticizer and foaming agent into a composite protein melt, which was heated in a hot mould (two parallel, heat controlled plates) to initiate the gas formation and foaming process.

A mathematical model for the foam density, based on the main ingredients and the mould temperature, was developed and verified. Analysis on both dough and foams were performed.

Specific measurements were performed on two different mixtures, identified by the model in having equal density but quite different structure. Foam characteristic (geometry, mean volume-weighted star volume, surface density and compression test) and rheological properties of the melt (extensional viscosity and strain hardening index) of these two were analyzed to further elucidate the relationship between the ingredients, and the process parameters and the foam and melt properties.

The percentage of zein/starch amount was the most important factor followed by the presence of foaming agent and the mould temperature respectively, while plasticizer was not important for the foam structure, even if it was necessary to form a melt at the process temperature.

The foaming process of dough with lower amount of zein was influenced by the swelling of starch, whose rate was related to the mould temperature, where the foaming agent was necessary to develop gas bubbles.

KEYWORDS: zein, starch, foaming process, model, extensional viscosity, strain hardening.

TABLE OF CONTENTS

1. INTRODUCTION

Foamed materials are currently used in different fields and applications: from packaging to insulation, and in food and biomaterials.

Besides the physical and chemical properties of the materials, cell structure is crucial, different cells size lead to different insulation and mechanical properties and even to different texture.

Thus, these properties could be modified by varying the percentages of the main ingredients and process parameters such as the foaming temperature, in other words by controlling the foaming process.

This work was focused on a cereal foam made of the protein zein, maize starch, plasticizer and foaming agent. The materials were first mixed together, in the right proportions, with distillate water to form a melt and then introduced into a hot mould (two parallel, heat controlled plates) were the foaming process took place.

This foam model was developed and characterized in order to investigate how the materials and process parameters affected the foam properties. A mathematical model able to predict the foam density was developed based on and measurements on both melt and foam. The foam structure was characterized by the analysis of sample sections and compressive testing and then the foaming properties of the melt were determined by hyperbolic contraction flow testing.

2. BACKGROUND AND THEORY

2.1. Zein

Maize (Zea mays) from the discovery of the Americas became one of the most common cereal in the world, nowadays it is second only to wheat and rice, and despite its poor nutritional quality it has been used as food (Arendt and Dal Bello, 2008).

As a matter of fact it is well known as the pellagra disease, common among the people whose diet was based on corn and sorghum, is provoked by a lack of vitamin B or tryptophan, the essential amino acid.

Its dominant protein class, zein, is particularly rich in glutamic acid (21-26%), leucine (20%), praline (10%) and alanine (20%) but deficient in lysine and tryptophan.

Thanks to its high content of praline and glutamine, zein could be classified into prolamin, and, since is a mixture of different peptides, could be divided into four groups based on solubility: α, β, γ and δ-zein.

The most abundant, α-zein (approximately 80%), is defined as the prolamine soluble in 95% ethanol and has a molecular weigh of 19-22 kD (Lawton, J.W., 2002); γ-zein (20%) needs a solution of aqueous ethanol with reducing agents in order to breake the disulphide bridges created by its cysteine amino acids (16-27 kD), (Shukla and Cheryan, 2001) while β (5%) and δ-zein have both a lower molecular weigh (so they require a less concentrated solution of ethanol) and are rich of methionine which as the cysteine is able to form disulphide bonds.

Extraction of zein is usually performed with a polar solvent such as aqueous isopropanol or ethanol at alkali conditions in order to increase its solubility; the process is commonly repeated several times to increase the purity of the zein. To this purpose a non polar solvent could be used such as hexane.

Isopropanol, being solubilised, also decreases the amount of β-, δ-, and γ-zein which yields a higher content of α-zein (Shukla and Cheryan, 2001; Lawton, 2002)

Since its isolation (John Gorham 1821), zein has been of scientific interest because of its insolubility in water, but only in the 20th century, due to the development of technology it has found applications in many fields like adhesive, biodegradable plastics, coating, fibers etc (Shukla and Cheryan, 2000).

Zein is insoluble in water alone (Lawton, J.W., 2002), like all the amorphous macromolecules, because of its structure is viscoelastic above its glass transition temperature (T_g) which can be lowered by adding a plasticizer.

The simplest kind of plasticizer is water; several studies have shown that the T_g of zein decrease rapidly with increase water content but, since this amount couldn't be as high as necessary, another kind of plasticizer is needed (Lawton, J.W. 1992).

In this way it is possible obtaining dough at rather low temperature.

2.2. Starch

Starch is the most important reserve of polysaccharide and the most abundant constituent in many plants including cereals.

It is constituted mainly by two different glucose polymers, amylose and amylopectin, which represent the 98%-99% of its dry weigh; the amount left is generally made up by integral lipids, small quantities of minerals and others substances, like lipids and proteins derived from the amyloplast membrane and non-starch sources.

Amylose is a linear polymer of α-1,4-linked D-glucopyranosyl units, largely 500-6000 glucose residues, with some branches of α-1,6-linkages; instead amylopectin has a similar structure but is a highly branched with a degree of polymerisation of $3 \times 10^5 - 3 \times 10^6$ units (Goesaert *et al.,* 2005; Richard *et al.*, 2004).

The bond difference leads to the structure of the starch, which nowadays is represented with the cluster model: a succession of amorphous and semi-crystalline rings.

In fact the amylopectin consist mainly of packed double helices alternated by the amorphous lamella of amylose.

The ratio between these two polymers vary depending on the botanic source: typical levels are 25-28% and 72-75% for amylose and amylopectin respectively (Richard *et al*., 2004).

The behaviour of this polysaccharide may be divided into three different processes: the moisturizing, the gelatinisation and the retrogradation.

The first one is reversible below a characteristic temperature, temperature of gelatinisation; added water to starch, it absorbs up to 50% of its dry weigh. If this mixture is heated above that point, it undergoes a series of changes that provoke loss of crystallinity, swelling of the granules, dissociation of the amylopectin double helices and leaching of the amylose. In case the heating process continues above the T_g, a starch paste is formed, characterized by a matrix of solubilised macromolecules of amylose in which is present a phase of swollen amorphous starch granules, containing mainly amylopectin.

Retrogradation occurs when the hot mixture is cooled below the T_g and the polymers reorganize into a more ordered and crystalline form, in fact the amylopectin molecules are able to reform double helices among a amylose phase, even if this may take days or week.

The behaviour of starch is fundamental both in bread and foam making: during the mixing the starch absorbs water and its main function is to act like a filler in a protein matrix, while in baking the granules swell and gelatinise combining to bring the volume and the initial firmness of the product (Goesaert *et al.,* 2005).

During the storage it, instead, retrogrades and is responsible for the staling process and the stiffness of the bread.

The main source of the world starch production is corn with the 80% of the total production. It may be developed in different types: starch with high amylose content (50-80%) and "waxy" starch in which this polymer is less than 5% of the total amount.

The size of such granules is typically from 5 to 30 μm in diameter (Arendt and Dal Bello, 2008).

2.3. Plasticizers

A plasticizer is an additive whose aim is to increase the flexibility, workability and distensibility of the phase in which it is added by reducing the melt viscosity, lowering the temperature of a second order transition (T_g) and the elastic modulus of the product (Raymond and Donald, 1953).

In the nineteenth century three different theories about the effects of plasticizers have been proposed; even if the first two are primitive and have been disproved in 1869, they are very useful to understand what the free volume theory shows.

The lubricity theory, the first one, considers plasticizers acting like oil between two moving parts; thus the resistance of a resin to deformation is provoked by intermolecular friction whose effect is minimized by a lubricant, which facilitates the movements of macromolecules over each other.

The second one is the gel theory; this considers the rigidity of a resin resulting from a threedimensional honeycomb structure developed by the attachments between the macromolecules: the closer and more numerous are, the stiffer or more brittle resin is. According to this theory the plasticizer acts breaking the attachments at places and masking the binding sites.

A more advance approach is stated by the free volume theory that investigates "what lies between the molecules and atoms".

The free volume or free space (V_f) in a crystal, glass or liquid, defined as the difference in volume between the one measured at absolute zero temperature (V_0) and the one found at a given temperature (V_t), is responsible for the rigidity or flexibility of a resin; i.e. a crystal has less free space in its structure than a liquid.

So the addition of plasticizer to a resin or to a dough improves its workability by increasing its free volume (Sears and Darby, 1982).

2.4. Foams and foaming agents

Foams are dispersion in which air or other gases forms the dispersed phase, and a liquid or solid the continuous phase (Raymond and Donald, 1953).

Some example like coffee foam, shaving foam or bread could make it easier to understand how common they are.

In order to form a foam, a gas should be mixed to the other phase which can be performed in different ways: mechanically or with the addiction of additives.

Injection under the surface, beating or occlusion under a stream of impinging on a liquid is examples of the first kind.

Foams can also be generated by the introduction of blowing agents (Sears and Darby, 1982) which could be both physical and chemical.

A physical blowing agent is, for example, a gas that expands after being forced into a continuous phase at high pressure while, a chemical, one is an addictive that decomposes over a certain temperature range, e.g. ammonium salts (baking powder).

2.5. Foam Characterization

The morphology of the two different phases and how these two are distributed is included in foam characterization.

A first interesting factor is the foam density (ρ_f) [Kg/m^3] simply calculated as the ratio between weight and volume of the foam sample. This index is not completely correct if the target is comparing two different foams obtained with two different polymers. It should be clear how the polymer density (ρ_p) might influence it.

For this reason the foam relative density is defined as (NJ Mills, 2007):

$$R = \frac{\rho_f}{\rho_p}$$ (Eq.1)

When no other phases are present, R is the volume fraction of polymer in the foam. Ceramicists prefer the concept of porosity, which is defined as (NJ Mills, 2007):

$$Porosity = 1 - R \qquad \text{(Eq.2)}$$

Obviously good information about the foam properties can be detected by studying the geometry and the shape of the cells.

For each cell is possible to detect a list of factors like:

- **Area** [mm^2];
- **Perimeter** [mm];
- **Aspect ratio**: the maximum ratio of width and height of the rectangle bounding the bobble;
- **Convexity**: the fraction of the measured cell's area and the area of its convex hull;
- **Diameter maximum** [mm]: the maximum diameter of a measured object;
- **Orientation** [˚]: the angle between the line corresponding to the maximum moment of the cloud of scaled points describing the cell and the X-axis.

Moreover information about the distribution of the two different phases inside the foam can be detected using stereology, the science of the geometrical relationship between a structure that exists in three dimensions and its image that is fundamentally two-dimensions (Russ and Dehoff, 2000).

The size of a discrete three-dimensional object, such as a particle or a cell, can be described using the mean volume weighted star volume.

The star volume of an object, with respect to an internal point, is the volume of the object seen unobscured from that point, this means that generally the star volume is less than the real one. Now if that point moves freely inside the object and the average is taken we obtain the volume weighted mean star volume (Reed and Howard, 1997).

It seems that the only problem is how to switch from two-dimensions to three and this is overcome with the intercepts method developed by Gundersen and Jensen (1985). It consists on a grate of lines lying upon the object and randomly translated, from which all the chords (l_0) are detected and measured (Fig.1).
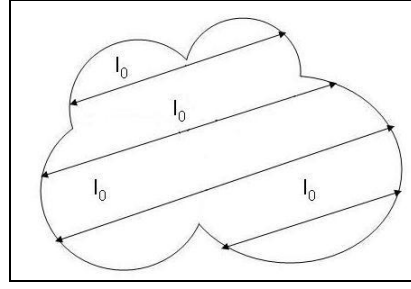
Figure 1. Schematic representation of the intercepts model.

And the mean volume-weighted star volume is estimated as (Reed and Howard, 1997):

$$\bar{v}_V^* = \frac{\pi}{3} \cdot \bar{l}_0^3 \qquad \text{(Eq.3)}$$

Where $\bar{l}_0^3$ is the average of the cubed lengths of the chords detected; good practice suggests that these should be approximately 200.

Another interesting value coming from stereology is the surface density value; it expresses the amount of surface area S(a) of a class of objects (a cell in foam for instance) contained in the unit containing tissue volume V(c), i.e. (Weibel R. Ewald, 1980):

$$S_{Va} = \frac{S(a)}{V(c)} \qquad \text{(Eq.4)}$$

To obtain such a value it is necessary to section the sample and work on the resulting image; like before, lines are placed on the section and they intercept the surface of the targeted object.

The intersection density I_{La} is the relationship between the numbers of intercepts I(a) and the line length in the tissue (Weibel R. Ewald, 1980):

$$I_{La} = \frac{I_a}{L_c} \qquad \text{(Eq.5)}$$

Moreover, it has been demonstrated that these parameters are proportional to each other and it is found that (Weibel R. Ewald, 1980):

$$S_{Va} = \frac{S(a)}{V(c)} = 2I_{La} = 2\frac{I_a}{L_c} \qquad \text{(Eq.6)}$$

2.5.1. Compressive test

Compressive tests, based mainly in deforming a sample with a compressive load, are used to investigate foam properties which are related to its structure.

The results are generally expressed in terms of stress, the load divided the cross section area, and strain, the sample deformation. A general curve of $\sigma(\varepsilon)$ (Fig. 2) presents three different zones: linear, cells collapse and densification region (Gibson and Ashby, 1997).
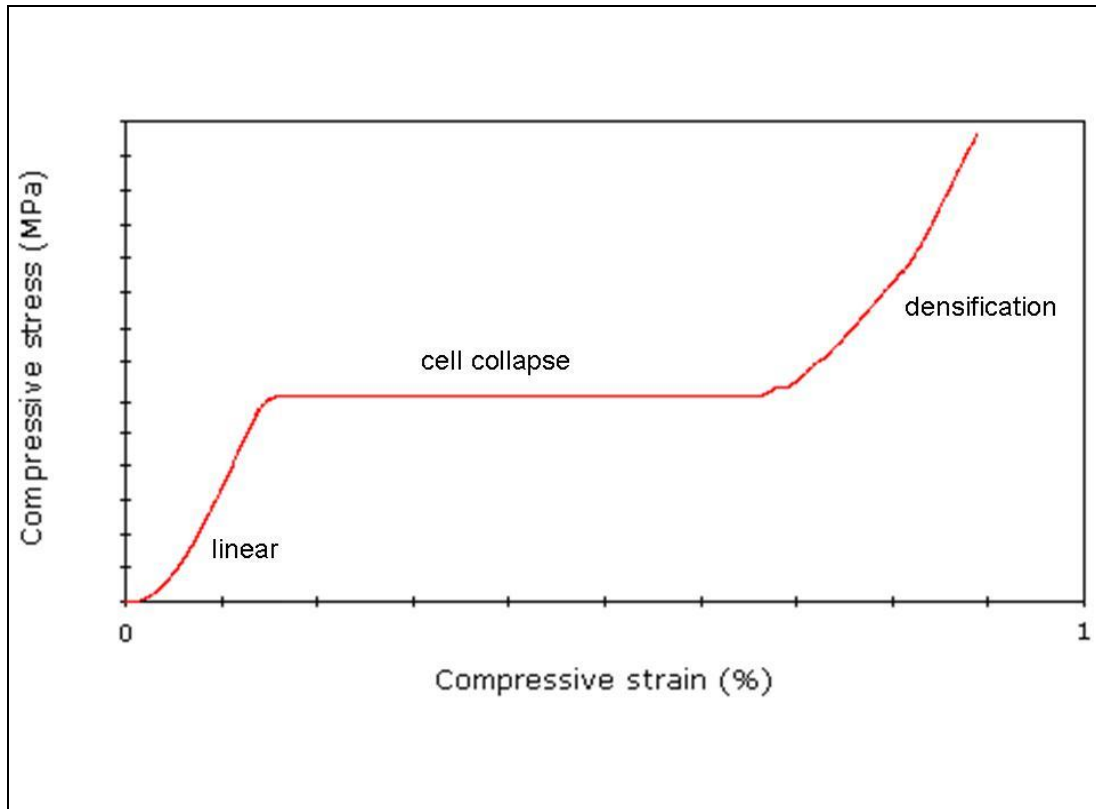

Figure 2. Compressive test's plot.

In the first part of the plot, the foam has a linear elastic behavior controlled by the cell wall bending and face cell stretching, here the Young's modulus, E^*, can be detected and represent the initial slope of the stress-strain curve.

Under an increasing load the curve reaches a plateau; here the cells start collapsing by elastic buckling, or by plastic hinges or by brittle crushing depending on the kind of foam. When the cells are almost completely collapsed and their walls are touching each other, the densification zone starts where the stress rapidly increases (Gibson and Ashby, 1997).

This plot gives also information about the energy absorbed by the foam during the test; in fact it's represented by the area embraced by the curve.

Increasing the relative density increases the Young's modulus, reduces the strain at which densification starts and raises the plateau level of the cell collapse region (Gibson and Ashby, 1997).

2.6.   Design of experiment

An experiment has been defined as an investigation of a process by changing inputs to the process, observing its response to the change, and inferring relationship from those observations (Sleeper D. Andrew, 2005).
It's clear how this can be run in very different ways, but an inescapable condition is efficiency, which means no waist of time and resources; for this reason planning at the desk is really important.

To make it more understandable what is written later a short list of definitions is necessary:

- a **factor** is a process input variable;
- a **level** is one setting of factors;
- a **response** is a process output;
- an **experimental unit** is a physical part of the process that varies or changes from trial to trial within the experiment;
- a **IPO structure** of an experiment is a description of the inputs (factors and levels), process (experimental units) and outputs (responses);
- a **screening experiment** has the target of testing several factors;
- a **modeling experiment** has the objective of developing a model for the process that reliably predicts future performance;
- a **trial** is one application of specific factors levels to the process;
- a **run** is a distinct combination of levels for all factors in an experiment;
- the **treatment structure** of an experiment is the assignment of factors and levels to the run of experiment;
- **replication** is the process of conducting multiple trials for all runs in an experiment.
- the **design structure** of an experiment is the assignment of experimental units to the trials in an experiment (Sleeper D. Andrew, 2005).

2.6.1. *The factorial design – Two level experiments*

Many experiments involve the study of the effects of two or more factors. In general, factorial designs are most efficient for this type of experiments; a factorial design means that in each complete trial or replication of the experiment, all possible combination of the levels of the factors are investigated (Montgomery C. Douglas, 2001).

Two levels experiments instead means that the factors' influence on the process is assumed linear and for this reason is possible to test only with setting of factors positioned on the sides of the system, which are two; for example the lowest and the highest values of a variable such as temperature.

The relatively easy analysis of this kind of experiments is possible only because they are orthogonal that means that all effects in the experiment can be estimated independently of each other.

Even if at first sight this way could seem not efficient and many people believe that that the best treatment structure is to changing one setting at time, this is the most natural end efficient way.

If for example we consider a process made up of three factors (A, B and C), the pictures below (Fig.3), representing the comparison between the two different structures, CEO method (change every thing at once) and COST method (change one setting at time) will show why.
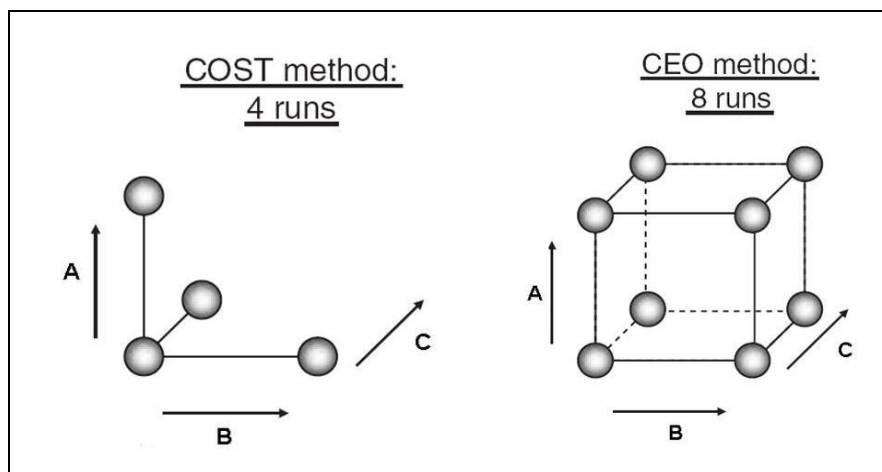

Figure 3. Comparison between COST and CEO method (a) (Sleeper D. Andrew, 2005).

From these pictures it seems that the only advantage of using the CEO method is the possibility of investigation a bigger space and eventually detecting all the two-factor interactions; and thus if those aren't present it seems a big waist of time and resource.

But if we think that a system is affected by noise and whereupon we need replications to obtain an average value of the main effects, is clear that the CEO method estimate it with four replications (Fig. 4).
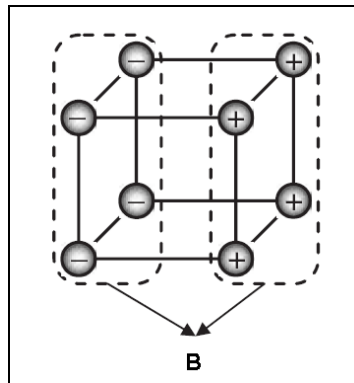
Focusing on the factor B:

Figure 4. Main effect's estimation (Sleeper D. Andrew, 2005).

The average value is calculated among four points on the left, the lower values, and the four on the right, the higher ones.

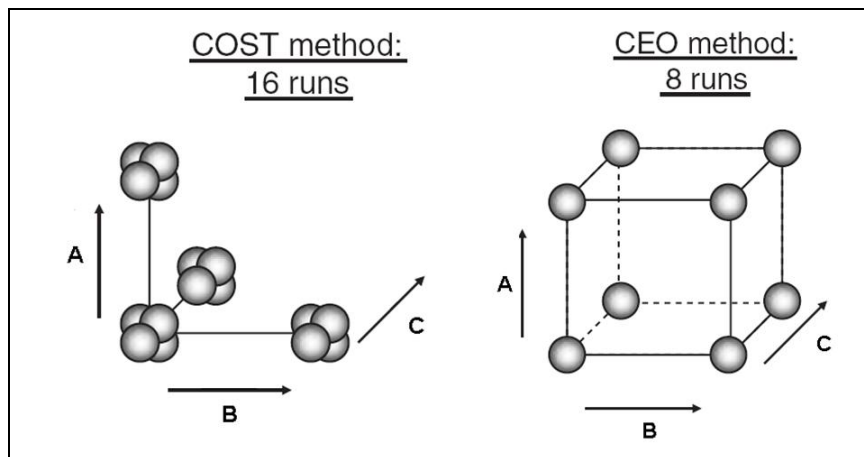So other pictures (Fig. 5) compare properly the two methods:

Figure 5. Comparison between COST and CEO method (b) (Sleeper D. Andrew, 2005).

Now even the most sceptics are forced to understand that this is the most efficient way possible.

As mentioned above, in this case the structure chosen is a full factorial which means that all the combinations of the levels of the factors are investigated (e.g. 3 factors and 2 levels means 2^3 runs); it's clear that with an increasing number of factors the system will became exponentially complex, that's why another kind of structure exists (fractional factorial), but is not interesting for this work.

Moreover to decrease the effects of the noise and to figure easily out if the process is not orthogonal some insurance policy must be taken: to prevent noise is necessary operate with

randomization and using replications (a good rule is to add 32 to number of runs and divide with the number of runs), while looking at the distribution of the residuals in their plot is a good way too understand if the process is not orthogonal.

The simpler experiment analysis can be done manually but there are a lot computer programs (MINITAB or DESIGN EXPERT for instance) that are really easy to use and give automatically results that however need to be interpreted.

Once decided the structure of the system and introduced all the data collected, the program will operate an ANOVA analysis (with a fix level of confidence, generally 95%) and all the results will be available to the operator.

The ANOVA could be interpreted by means of the PARETO chart and the R^2 and R^2 adjusted values; in the first one where the p-values of the factors and their interactions are showed while the second value is referred to how much the model fits the process (the closer to 100% the better). The adjusted R^2 value instead includes the penalty for having more terms in the model, thus this value is better to compare different models.

Moreover all of these programs are able to generate automatically a randomization way to make all the different runs and other plots like the residuals plots (Standardized Residual, Fitted Values, Observation Order…), cube plot and interaction plot.

The fact that the relationship between factors and results is supposed to be linear, leads to a linear model, whose coefficients are calculated by means of the ANOVA, and this is just a linear combination of the factors; for example:

$Y = b + b_1X_1 + b_2X_2 + b_3X_3 + b_4X_1X_2 + b_5X_1X_3$

Where Y is the response, X is the factors and b is the coefficients.

Real processes are rarely exactly linear, but an estimated linear function is often close enough to be useful (Sleeper D. Andrew, 2005); anyway when the process performance is very nonlinear it could be very inaccurate.

The most inexpensive way to figure it out is adding centre point runs to a two–level treatment structure: for linear system the centre point's value will be the same as the average response of the corner points, otherwise a significant difference among them will indicate the presence of non linear effects (curvature).

2.6.2. Three levels experiments

To investigate nonlinear process one more level could be add, this should be enough for almost every experiments; thus models derived from three-level experiments may include quadratic terms in addition to linear terms and interactions.

Efficiency is more even important here, if for a two level experiment with four factors are necessary 16 runs, with a three level with the same number of factors are 81!!

Luckily, beyond full factorial, three other different treatment (Fig.6) structures with positive and negative aspects are available: Taguchi L9, Box-Behnken and Central Composite.
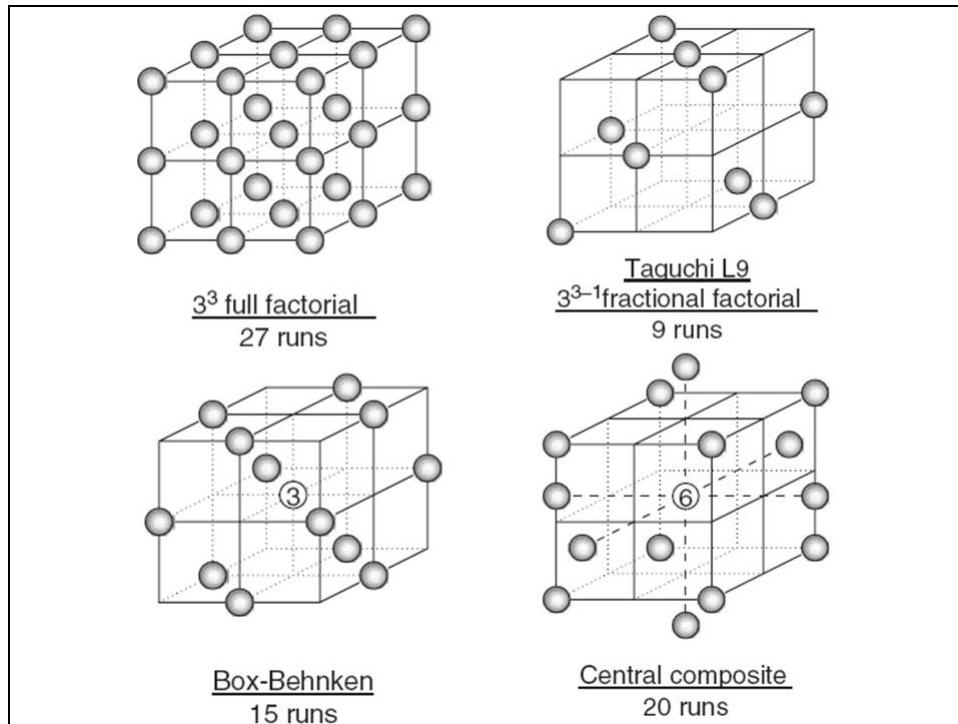

Figure 6. Three level treatment structures (Sleeper D. Andrew, 2005).

The full factorial treatment structure contains all the different combinations of factors and, for this reason, has a low efficiency; the Taguchi instead is a fractional factorial structure and the model from this experiment includes only quadratic and main effects (is indicated when the system is known in advance to be nonlinear), The Box Behnken's model has only the quadratic terms and linear interactions and has the advantage to avoid corner points.

But the most popular structure is central composite because it contains corner points like a two-level factorial experiment, plus axial points (set up with a α index), plus centre points.

So in phase one is possible to conduct a two-level factorial design with centre points and, if the system shows a nonlinear behavior, is possible to extend the experiment to a central composite structure, phase two, adding axial points and other corner points (Sleeper D. Andrew, 2005).

It could be difficult to find the different combinations of factors' values that belong to each point, but using the pc's programs mentioned above is pretty easy: they do it automatically once selected the treatment structure, the number of factors and their higher and lower values.

Obviously every model derived from this kind of analysis must be verified.

2.7.   Rheology

The term rheology originates from the Greek "rheos" meaning the river; thus rheology is literally the "flow science" or, in a better way, is defined as the study of the deformation flow of materials (Barnes, H.A, 2000).

These are investigated by giving them some controlled deformations under fix conditions (time, temperature, pressure, etc…) and studying the response; this leads to information about the material properties.

It's really important to present the following definitions:

- **Stress**: is the total applied force (F) per unit area (A) that causes deformation or flow.
- **Strain**: is the relative measure of the deformation, it's called relative because is referred to a fix state, generally the initial.
- **Strain rat**e: is the rate at which material is deformed.
- **Modulus**: is an expression of the rigidity/stiffness of the material, which relates to the stress and the strain.
- **Viscosity**: is a measure of the resistance to flow, in fact relates the stress and the strain rate.

Deformation can be divided into shear and extensional or compressional deformation; in shear deformation (Fig. 7) the force in applied parallel to a surface while in the other case (Fig.8) the force is perpendicular to the surface which is related to.

All the equations describing the relationship between properties are similar and are listed below:
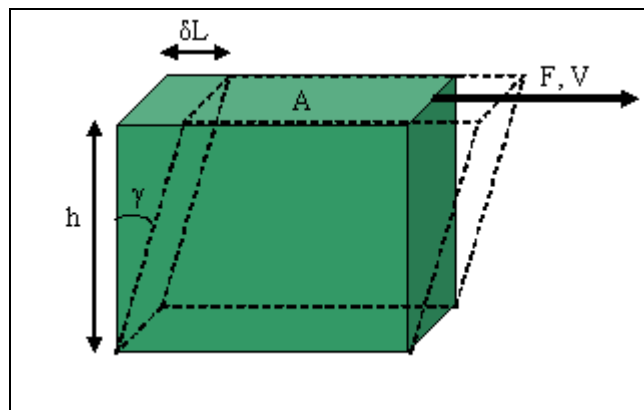

Figure 7. Shear deformation.

For shear:

F: force [N]

V: speed [m/s]

A: area [m^2]

h: high [m]

δL: shear displacement [m]

Shear stress: $\tau = \dfrac{F}{A}$ [Pa] (Eq.7)

Strain: $\gamma = \dfrac{\delta L}{h}$ (Eq.8)

Shear rate: $\dot{\gamma} = \dfrac{V}{h}$ [1/s] (Eq.9)

Shear viscosity: $\eta = \dfrac{\tau}{\dot{\gamma}}$ [Pas] (Eq.10)

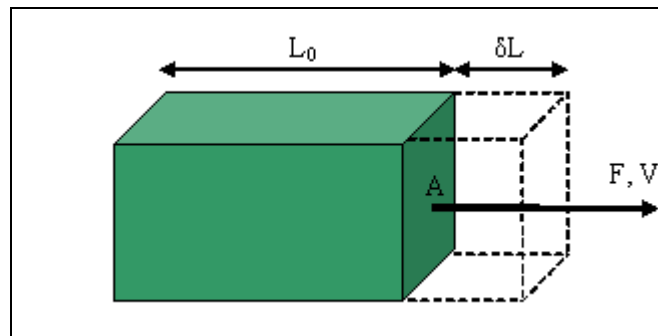Elastic shear modulus: $G = \dfrac{\tau}{\gamma}$ [Pa] (Eq.11)

Figure 8. Extension deformation.

For extension:

F: force [N]

V: speed [m/s]

A: area [m^2]

L_0: initial length [m]

δL: elongation [m]

Tensile stress: $\sigma = \dfrac{F}{A}$ [Pa]   (Eq.12)

Cauchy strain: $\varepsilon = \dfrac{\delta L}{L_0}$ (Eq.13)

Extension rate: $\dot{\varepsilon} = \dfrac{V}{L_0}$ [1/s]   (Eq.14)

Extensional viscosity: $\eta_E = \dfrac{\sigma}{\dot{\varepsilon}}$ [Pas]   (Eq.15)

Tensile elastic modulus: $E = \dfrac{\sigma}{\varepsilon}$ [Pa]   (Eq.16)

Materials can be divided into three different families: Hookean elastic solids, Newtonian liquids and viscoelastic materials.

The first ones are described formally using the Hook's law and its behaviour is generally represented by a spring: under a constant force it shows immediately the corresponding deformation and keeps it as long as the force is acting, while, when the load is uncharged, it returns to its original shape without any permanent deformation (Mezger, T.G., 2006).

Hook's law:

$$\sigma = E \cdot \varepsilon \ \text{(extension)} \quad \text{or} \quad \tau = G \cdot \gamma \ \text{(shear)} \qquad\qquad \text{(Eq.17)}$$

Where G or E represent the direct proportionality between the stress (tensile or shear) and the strain and could be compared to the spring constant.

Thus the spring as well as the Hook's solid stores energy and has an elastic behaviour.

Newtonian's liquids instead could be represented by a dashpot: the deformation is related to the rate of force and when the load is removed the shape remains permanently changed; in this case an irreversible process has taken place and the energy is dissipated as heat (Mezger, T.G., 2006).

$$\tau = \eta \cdot \dot{\gamma} \qquad\qquad\qquad\qquad\qquad\qquad\qquad\qquad\qquad\qquad \text{(Eq.18)}$$

Where η is the shear viscosity and represent the relationship between the stress and the strain rate and could be used as the dashpot constant.

It's clear that these are two ideal states and that most materials have both elastic and liquid properties and are called viscoelastic.

Different models have been proposed but the most popular are the Maxwell (Fig. 9) and the Kelvin/Voigt's ones (Fig.10) in which the spring and the dashpot are combined in different ways.
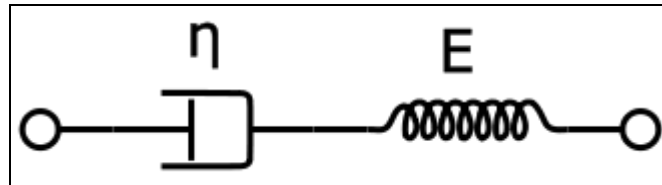

Figure 9. Schematic representation of Maxwell's model.

In the first one, a spring and a dashpot are connected in series and the final deformation is the sum of the two element's ones.
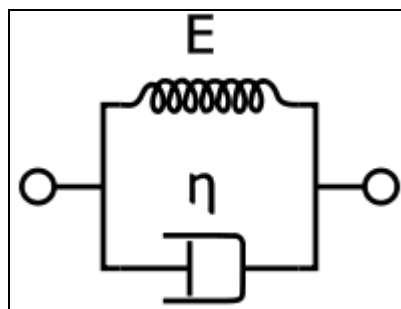

Figure 10. Schematic representation of Kelvin/Voigt's model.

In Kelvin/Voigt's model a spring and a dashpot are connected in parallel and the final stress is the sum of the two elements.

By combining these two simple models others were developed, like the Maxwell-Weicher's.

2.7.1. Non Newtonian materials and Power law

Newton's law describes only a particular kind of fluids, the ones whose viscosity is constant, there are others that show a different behaviour. The simplest are called shear-thickening, if the viscosity increases, or shear-thinning, if the viscosity decreases with strain rate.

Examples of shear-thinning could be polymers solutions, polymer melts, many paints, glues and shampoos while examples of the other could be ceramic suspensions and starch dispersions (Mezger, T.G., 2006).

The "Ostwald-de Waele power-law" for shear flow is able to describe both fluids (Barnes, H.A., 2000):

$$\sigma = K\dot{\gamma}^{n} \tag{Eq.19}$$

or

$$\eta = K\dot{\gamma}^{n-1} \tag{Eq.20}$$

Where K and n are, respectively, the consistency index and the power-law index (Barnes, H.A., 2000) and can be determined with oscillatory or rotational measurements in the linear viscoelastic region (LVE). Newtonian liquids have n=1 and K equal to the viscosity, now the power-law is the same as the Newton law; instead shear-tinning materials have n<1 while shear thickening ones have n>1 (Fig. 11).
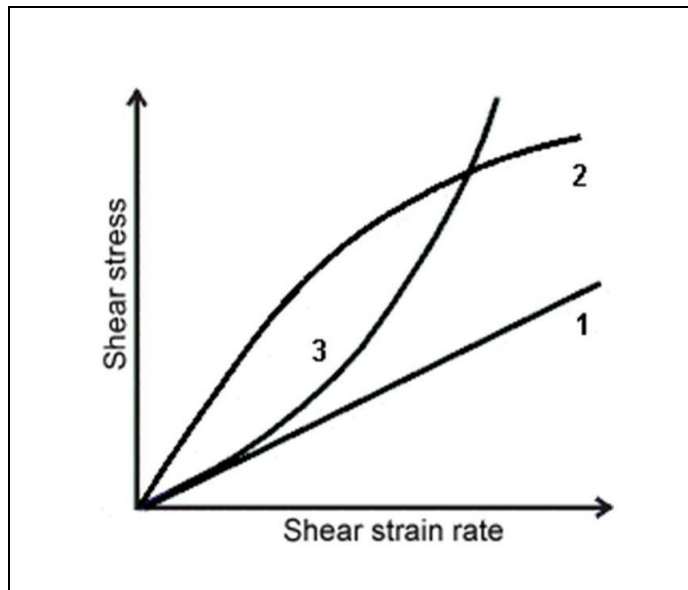

Figure 11. Fluids' behaviour. 1- Newtonian, 2- Shear-thinning, 3- Shear-thickening.

2.8. Oscillatory measurement

Oscillatory measurements are used to examine all kinds of viscoelastic materials, from low-viscosity liquids to polymer solutions and even rigid solids (Mezger, 2006), but are more

appropriate for elastic liquids, such as dough, since rotational measurements would compromise their structure (Barnes, 2000).

The sample is e.g. kept between two discs, one stationary and one oscillating, subjected to a sinusoidal deformation at a particular angular frequency (ω), while the response is registered as represented by these equations:

$$\gamma = \gamma_0 \sin(\omega t) \tag{Eq.21}$$

and

$$\tau = \tau_0 \sin(\omega t + \delta) \tag{Eq.22}$$

Where t is time, ω the angular frequency, δ is the phase shift angle and τ_0 and γ_0 are the amplitudes of shear stress and strain, respectively (Fig.12).
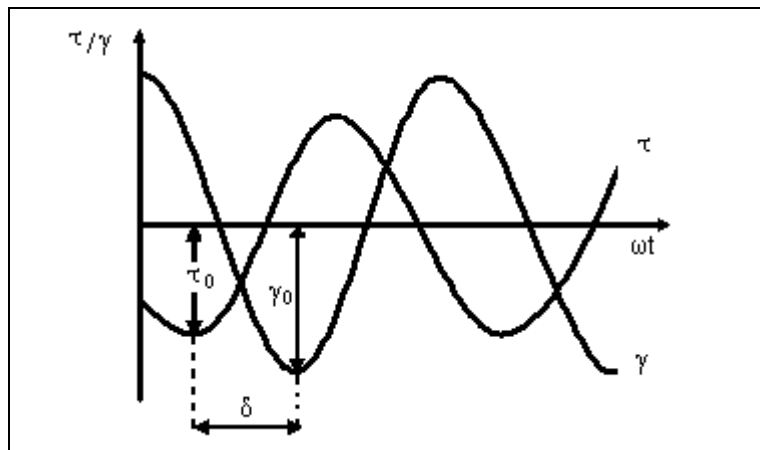
Figure 12. Stress/strain-time plot.

Inferring relationship between inputs and outputs gives information on the material's properties; in fact δ connects stress and strain.

An ideal elastic sample would respond immediately to its deformation and the phase angle would be 0, while an ideally viscoelastyc one would have the maximum delay possible, that is π/2 rad (=90˚).

As should be clear at this point, a real material lies among these two extremes.

To figure out how much a material is elastic or viscous another equation should be introduced:

Loss factor: $\tan \delta = \dfrac{G''}{G'}$ (Eq.23)

Where G' is the storage modulus, a measure of the deformation energy stored that is completely available when the load is removed; and G'' is the loss modulus, a measure of the deformation energy dissipated during the shear process. Thus G' represents the elastic behaviour of the material, while G'' the viscous one (Mezger, 2006).

It's of easy understanding why when δ=0 the G''=0.

These two form together the shear complex modulus (G*), that is represents the material's stiffness or rigidity to this kind of deformation.

These are related by the following equations:

$$G* = G' + iG'' \qquad\qquad i^2 = -1$$ (Eq.24)

$$\left| G* \right| = \sqrt{(G')^2 + (G'')^2}$$ (Eq.25)

Is also possible focusing on the strain rate and its effects; it's the time derivate of the strain, so its equation is the one below (Mezger, 2006).

$$\dot{\gamma} = \gamma_0 \omega \cos(\omega t)$$ (Eq.26)

And it is related to the stress due to the complex viscosity (different from the shear viscosity η), obtained applying the Newton's law (Mezger, 2006).

$$\eta* = \dfrac{\tau(t)}{\dot{\gamma}(t)}$$ (Eq.27)

Moreover the relation among complex viscosity and complex modulus is (Mezger, 2006):

$$\left| G* \right| = \omega \cdot \left| \eta* \right|$$ (Eq.28)

Obviously, performing this kind of tests, many parameters could be varied such as temperature, frequency and stress amplitude.

2.8.1. *Amplitude sweep and linear viscoelastic region (LVE)*

These test are performed at variable amplitude (it could be either stress or strain) while the frequency and the temperature are kept at constant value (Fig.13) (Mezger, 2006), instead the other parameter, G' and G'', are targets.

Figure 13. Amplitude sweep plot.
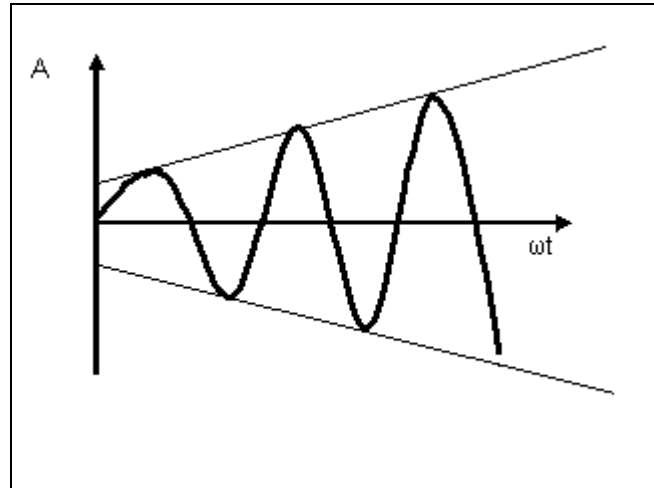
Usually this is the first measurement carried out since is necessary to find out the linear viscoelastic region (LVE) which is really important for further tests since, in this space and under this amplitude of deformation, both the Hooke's law and the Newton's law are valid (Mezger, 2006). This means that, in this region, G' and G'' should be constant and showing constant plateaus.

2.8.2. Frequency sweep and Cox-Merz rule

Frequency sweeps giving the mechanical spectrum are oscillatory tests performed at variable frequency (Fig.14), keeping the amplitude and the temperature constant (Mezger, 2006) and all the others parameters, complex viscosity first of all, are investigated.
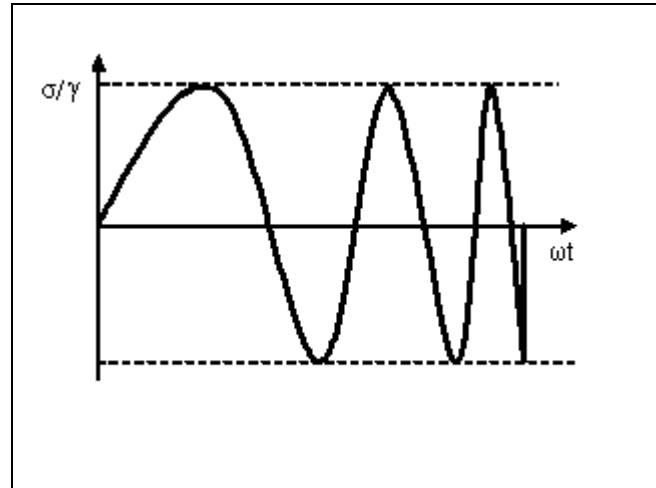

Figure 14. Representation of the frequency sweep.

The set amplitude is generally the one obtained from the previous test (amplitude sweep) in order to investigate the sample in its LVE (Fig.15) a particular region in which the empirical Cox-Merz rule is valid.

This law states that the complex viscosity and the shear viscosity are equal:

$$|\eta^*(\omega)| = \eta(\dot{\gamma}) \qquad \text{for} \quad \omega = \dot{\gamma} \tag{Eq.29}$$

Thus the liquid could be characterized whit the Power law and so is possible to find the consistency index (K) and the power-law index (n).

Since both the frequency and the complex viscosity are expressed in logarithmic scale the power law has this equation:

$$\ln\eta = \ln K + (n-1)\ln\dot{\gamma} \tag{Eq.30}$$

Where η [Pa] is replaced with $|\eta^*|$ and $\dot{\gamma}$ [1/s] with ω [rad/s];
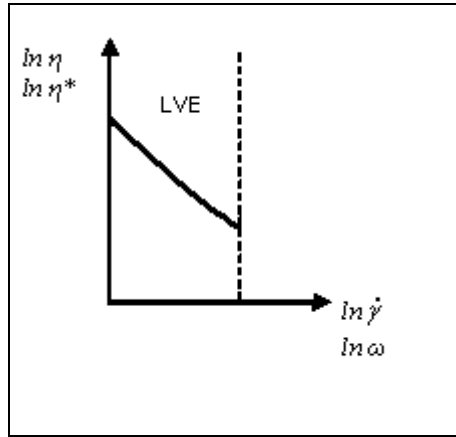
Figure 15. Viscosity in the LVE region.

Thus those constants could be calculated; the n is the slope of the diagram plus 1 instead the K is related to the intercept.

$$n = slope(\ln\eta; \ln\dot{\gamma}) + 1 \qquad\qquad (Eq.31)$$

$$K = e^{\wedge}(int(\ln\eta; \ln\dot{\gamma})) \qquad\qquad (Eq.32)$$

This relation is not useful for materials showing G'>G'' ("gel character") in the low-shear range, such as stable dispersions (Mezger, 2006).

2.8.3.   Temperature sweep and glass transition temperature

A temperature sweep measurement is a test in which both frequency and amplitude of the deformation are kept constant while temperature is the only variable parameter (Mezger, 2006).

The glass transition temperature (T_g) is a temperature at which a material changes its state, from a glassy state to a rubbery one. In terms seen in the previous paragraphs, this means that in the first state the macromolecules are almost frozen; thus the resulting solid is rigid and brittle and it shows a G'>G''. While in the rubbery state it G' is closer to G'' and exhibits the behaviour of a viscoelastic liquid (Mezger, 2006).

Since the tangent of the phase angle is the ratio between the storage and the loss modulus, the glass transition temperature could be determined searching a peak in the curve describing the phase angle (Schober et al., 2008).

2.9. Extensional viscosity

As seen in previous paragraphs, flow can be experienced both in shear and in extension and for this reason viscosity as well.

Focusing on uniaxial extension, which means that an element is compressed on two directions and free to extend in the one left (Fig. 16), the phenomenon is expressed by the following equations.
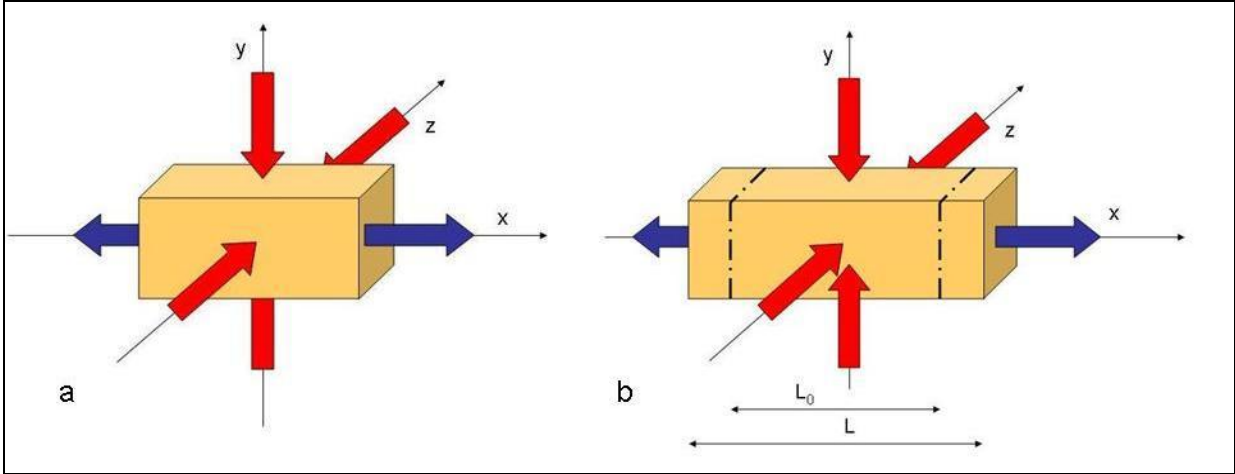
Figure 16. Uniaxial extension (a). Deformation after loading (b).

$$\text{Stress: } \sigma_E = \frac{F}{A} \qquad\qquad (Eq.33)$$

Where A is the surface area and F the force applied on;

$$\text{Strain: } \varepsilon = \frac{L - L_0}{L_0} \qquad\qquad (Eq.34)$$

$$\text{Strain rate: } \dot{\varepsilon} = \frac{V}{L} \qquad\qquad (Eq.35)$$

Where L is the final length and L_0 is the one at the starting point.

$$\sigma_E = \eta_E \cdot \dot{\varepsilon} \quad \Rightarrow \quad \eta_E = f(\dot{\varepsilon}) = \frac{\sigma_E}{\dot{\varepsilon}} \qquad\qquad (Eq.36)$$

Where η_E is the extensional viscosity, which can be considered the resistance of the material to this kind of deformation.

The fact the sample is squeezing while is deforming leads to two problems: the first one is that since the area (A) is decreasing the stress (σ) is increasing and the second one is that since length (L) is increasing the strain rate is decreasing.

Thus the extensional viscosity is dependent on both strain rate and time (Steffe, 1996).

$$\eta_E = f(\dot{\varepsilon}, t) = \frac{\sigma_E(t)}{\dot{\varepsilon}}$$

In order to keep constant the strain rate the sample must be extended exponentially (Barnes, H.A., 2000), or the measurement system must have a particular geometry, such as in hyperbolic contraction flow (Wikström and Bohlin, 1999b) Similarly to the shear viscosity, materials could be tension-thinning or tension-thickening depending on how the extensional viscosity changes with the strain rate and it does not correspond to the shear behaviour.

2.10. Strain hardening

Strain hardening is defined as the phenomenon when the stress required to deform a material increases more than proportional to the strain (at constant strain rate and increasing strain) (Van Vliet, 2008).

In foaming the dough is deformed in planar extension i.e. it is axially compressed and stretched in the other two directions, so this material's characteristic is fundamental to stabilize the walls and retain the gas; otherwise the lamella between two cells would have a premature rupture.

Thus materials with higher strain hardening have better foaming properties and prevent coalescence.

In uniaxial extension, strain hardening, is defined by the following relation:

$$\frac{d \ln \sigma_E}{d \ln \varepsilon_H} > 1 \qquad\qquad\qquad\qquad (Eq.37)$$

An empirical equation, called Hollomon equation, is commonly used to determine strain hardening from the experimental data from tests in uniaxial extension (van Vliet, 2008).

$$\sigma_E = A\varepsilon_H^m \qquad\qquad\qquad\qquad (Eq.38)$$

Where σ_E is the extensional stress, A is a constant (equal to σ_E for ε_H=1), m is the strain hardening index and ε_H is the extensional Hencky strain calculated as:

$$\varepsilon_H = \dot{\varepsilon} \cdot t \qquad \text{(Eq.39)}$$

The pom-pom model, proposed by MacLeish and Larson, describing the rheological behaviour of HMW branched polymers melts is a rather good way to clarify the strain hardening effect. According to this theory, polymers, described as to backbones with braches radiating out, bonded all together, form a net which produces a strain hardening effect in case those backbones are stretched (Dobraszczyk and Morgenstern, 2003). In uniaxial extension, strain hardening can be detected with contraction flow, while in biaxial extension with bubble inflation of dough sheet (Steffe, 1996).

2.11. Hyperbolic contraction flow

Hyperbolic contraction flow is a method to measure the uniaxial extensional viscosity and the strain hardening index during the start up period. The architecture of this device is simple and consists mainly in a load cell, a contraction nozzle, a feeding piston and a cylindrical sample cell. First the cylindrical sample cell is loaded with the sample and then the piston, moving at a constant speed, squeezes the sample through the nozzle while the load cell is measuring the stress. Since the nozzle is pressed against the load cell, the friction forces between the piston and the wall of the sample tube are not recorded (Wikström, Bohlin, 1999a). Obviously, while is resting, the sample does not show any stress or strain.

In measuring the extensional viscosity two different problems have to be faced.

The first one, keeping a constant strain rate while the sample is deforming, is solved thanks the nozzle's shape; the radius of the nozzle at any given point z along the nozzle height has to be (Wikström, Bohlin, 1999a):

$$r(z) = \frac{r_0}{\sqrt{\frac{z}{H} \cdot \left(\frac{r_0^2}{r_1^2} \right) + 1}} \qquad \text{(Eq.40)}$$

Where H is the nozzle height, r_0 is the inlet radius and r_1 is the outlet radius. Thanks to this relation the nozzle has a hyperbolic shape (Fig.17).
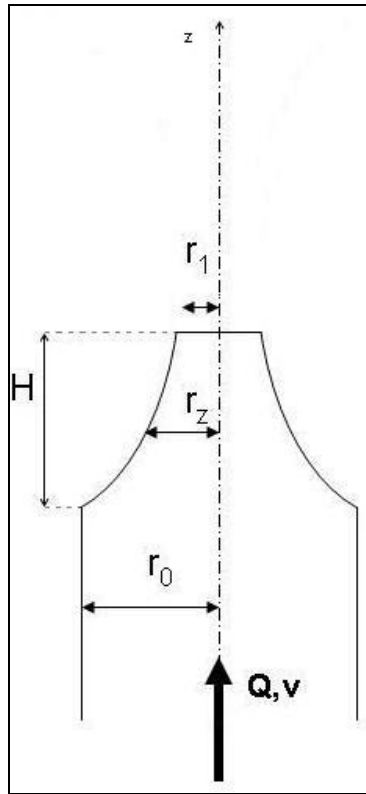
Figure 17. Nozzle shape.

Considering n as the power law index from shear flow, Q the volumetric flow and t the time it takes to transport a volume element from the inlet of the nozzle to the outlet, the following equations express respectively the constant strain rate and the Hencky strain (Wikström, Bohlin, 1999a):

$$\dot{\varepsilon} = \frac{3n+1}{n+1} \cdot (Q/\pi) \cdot \frac{r_1^{-2} - r_0^{-2}}{H} \qquad (Eq.41)$$

$$\varepsilon_H = \int \dot{\varepsilon}\, dt = \dot{\varepsilon} \cdot t \qquad (Eq.42)$$

Meaning that:

$$\varepsilon_H = \frac{3n+1}{n+1} \ln\left(\frac{r_0^2}{r_1^2}\right) \qquad (Eq.43)$$

At a given displacement and piston speed is:

$$t = \frac{H_{eq}}{v} \tag{Eq.44}$$

Where H_{eq} is the height of the sample tube having a volume equal to the volume of the nozzle, defined as (Wikström, Bohlin, 1999a):

$$H_{eq} = \frac{H \cdot \ln(r_0^2 / r_1^2)}{((r_0^2 / r_1^2) - 1)} \tag{Eq.45}$$

By combining equations 44 and 45 is possible to express the Hencky strain as (Wikström, Bohlin, 1999a):

$$\varepsilon_H = \frac{3n+1}{n+1} \ln\left(\frac{r_0^2}{r_1^2}\right) \tag{Eq.46}$$

By definition the extensional viscosity is the ration between the stress and the strain rate, where the stress can be calculated as the compressive load registered by the load cell (Ft) divided by the sample's area at the outlet point. That means (Wikström, Bohlin, 1999a):

$$\eta_E = \frac{\sigma_E}{\dot{\varepsilon}} \Rightarrow \frac{\dfrac{F_t}{\pi r_0^2}}{\dot{\varepsilon}} = \frac{\sigma_{meas}}{\dot{\varepsilon}} \tag{Eq.47}$$

This equation in not entirely true since the force measured (σ_{meas}) includes shear forces needed to squeeze the sample through the nozzle.

The value of shear can be estimate by calculating the shear stress (σ_{shear}) over the nozzle for a power-law liquid at a volume flow rate Q (Wikström, Bohlin, 1999a):

$$\sigma_{shear} = \frac{4H\left(3+\dfrac{1}{n}\right)^n \left(\dfrac{K}{\pi}\right)^n Q^n \left(\dfrac{1}{r_0^{3n+1}}\right)^n}{3n+3} \times \frac{\left(\dfrac{r_0^2}{r_1^2}\right)^{\frac{3n+3}{2}} - 1}{\dfrac{r_0^2}{r_1^2} - 1} \tag{Eq.48}$$

Now the uniaxial extensional viscosity can be determined:

$$\eta_e = \frac{\sigma_{corr}}{\dot{\varepsilon}} \Leftrightarrow \frac{\sigma_{meas} - \sigma_{shear}}{\dot{\varepsilon}} \qquad \text{(Eq.49)}$$

$$\eta_e = \frac{\sigma_{corr}}{\dot{\varepsilon}} \Leftrightarrow \frac{\sigma_{meas} - \sigma_{shear}}{\dot{\varepsilon}}$$

3. MATERIALS AND METHODS

3.1.   Materials and foam development

Zein (Moisture content, MC = 4.88% wet basis), and corn starch (MC = 11.84% wet basis), was purchased from Sigma-Aldrich (Stockholm, Sweden). Citrofol A1 (triethylcitrate, min. 99%) was from Jungbunzlauer (Ladenburg, Germany) and baking powder (ammonium carbonate E503) was produced by Santa Maria (Mölndal, Sweden).

The moisture content of zein and starch was determined by drying over night in an oven at 110 ℃.

Distilled water was added to the correct amount of these powder (see the following paragraphs) and a dough was formed using a 10g mixograph (ReoMixer^{TM}, Reomix Instruments, Lund, Sweden) at a movable average length of 40 and motor speed byte of 250.

Moreover, the total amount of flour was established of 10g and the quantity of zein and starch expressed in relation to the flour content.

The temperature of this process was set at 40℃, above the glass transition temperature of the zein, and kept constant by a water bath connected to the mixing beaker; the mixing was performed until the registered torque reached 9 Nm since the stiffness of the dough would have otherwise compromised the safety of the reomixer. This means that different recipes were mixed for different times to allow the same development of the protein network inside the dough.

The foaming process was performed by baking; the dough was heated inside a hot mould, two parallel, heat controlled plates (Appendix 1), for 40 minutes and to obtain a product with a disc shape, thick enough to notice the foam structure and round to consent a perfect bubble growing, an aluminium frame of 20 mm thickness and with a hole of 50 mm diameters was used (Appendix 2).

3.2.   Model structure and development

3.2.1.   Screening test and factors

Screening experiments has the objective of testing several factors and determining which ones have significant effects on the process; for these reason they were run before the model developing (Sleeper D. Andrew, 2005).

Through them the process was tested and an average recipe was found (5g of zein, 5g of starch, 0,3g of baking powder, 0,75g of citrofol A1 and 6,5g of distilled water) and four different factors identified.

The factors were recognized as the amount of zein/starch, of plasticizer, of foaming agent and the mould temperature; besides, due to other trials, their limiting values were determined as:

- **Zein**: [40%; 60%]. Because with a lower amount of zein the final product couldn't be considered foam, while with a higher one it was a shell.
- **Plasticizer** (Citrofol A1): [0.5g; 1g]. Because was not possible, with a lower amount, obtaining a dough, instead, with a higher one, in the bottom of the mixing beaker remained a little water and a little plasticizer as well.
- **Foaming agent** (baking powder): [0g; 0.6g]. Since achieving a dough was not possible with more foaming agent.
- **Mould temperature**: [120ºC; 200ºC]. Since at lower temperature the final product was still wet and collapsed during the storage and since at higher temperature the product began burning.

All the other possible factors, e.g. the mixing time and temperature and the baking time, were kept constant.

The final recipe and the process parameters are listed in the following table (Tab. 1).

INGREDIENT/PROCESS PARAMETER	VALUE
Zein	[40%; 60%]
Plasticizer	[0,5g; 1g]
Foaming agent	[0g; 0,6g]
Water	6,5g
Mixing temperature	40 ºC
Mixing time	Until the mixing torque reaches 9 Nm
Baking temperature	[120 ºC; 200 ºC]
Baking time	40'

Table 1. Summary of the process: ingredients and factors.

3.2.2. *Model structure*

Several responses were tested, such as cell sphericity, orientation and the Young's modulus deriving from compression analysis, but only the foam density (ρ_f) [Kg/dm^3] gave satisfactory results.

Since the different recipes used to create different foams led to polymers with a density that could be considered constant, foam density was preferred to relative density (R); moreover this value was easier and faster to be evaluated (Fig. 18). Volume and weight were measured after two days storage at constant temperature and humidity, respectively 23 ºC and 50%.

In phase one, as treatment structure, was chosen a two levels full factorial design with four factors and the addiction of four centre points to value the assumed linear relationship between factors and response.

Figure 18. IPO structure of the process.

Only one replication was done and the program used to generate the completely randomized design structure and realize a model was Design Expert 7.1.6. (Science Plus Group, Groningen, Nederland).

The program ran the data analysis and found out that the deriving model had a statistical significance, but anyway there was a strong nonlinear behaviour since there's a great difference between the average density value of the centre points and the average response of the corner points; thus this model could not be assumed as valid since it didn't fit correctly the process space, especially in the middle of the system.

For this reason a new treatment structure was chosen, phase two: three levels face centred central composite design.

This meant that 10 more runs were added, corresponding to 2 centre points and to 8 axial points lying on the face of the investigated space ($\alpha=1$), quadratic factors were investigated and thus the non-linear issue was overcome.

3.3. Foam characterization

Due to the model it was found that two different recipes led to different foam structures but had the same density.

The first one was: 40% zein, 0.5g of plasticizer, 0.6g of foaming agent, 6.5 g of distilled water and 120 ºC was the mould temperature.

The second one was: 60% zein, 0.5g of plasticizer, 0g of foaming agent, 6.5 g of distilled water and 120 ºC was the mould temperature.

Four runs each were made to confirm the model's prediction.

3.3.1. Image data analysis

After two days storage at 23 ºC and 50% R.H., three different samples per recipe were cut twice in a randomized way due to a simple program generated with Microsoft Excel.

It had returned three numbers per sample (Fig. 19): α, the angle necessary to find a main diameter (y), d, the distance between that diameter and the first cut, and β, the angle between the two cuts.
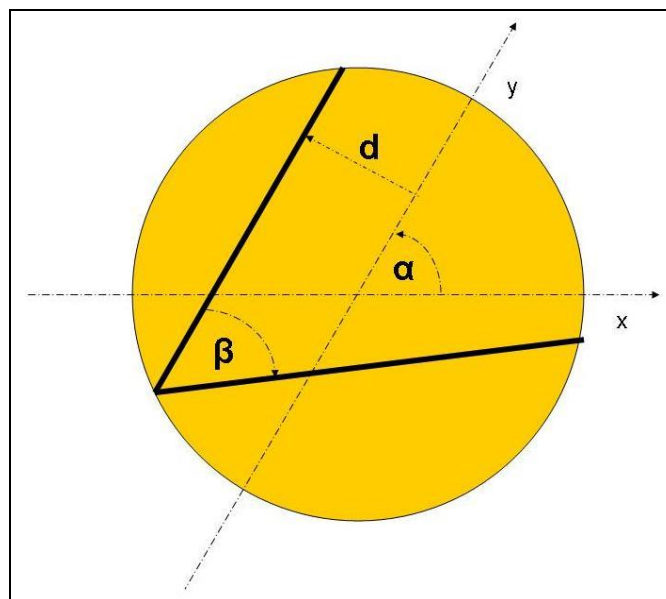

Figure 19. The randomized cuts (the lines in bold).

This was possible in reference to the first diameter (x), recognizable due to the frame used, and since the edges of those parameters were set as:

α: [0º; 360º];

d: [-20mm; +20mm];

β: [20º; 40º] towards the bigger piece left.

Thus six pictures per recipe were scanned with a Canon CanoScan N1240U scanner (Canon Inc., Tokyo, Japan) and analyzed due to AnalySIS (Soft Imaging System).

A sequence of filters and actions (in order DCE, the color separation of green, binarizition and the morphological filter of erosion) was used to fix the images (Fig. 20 and 21) to the further analysis.

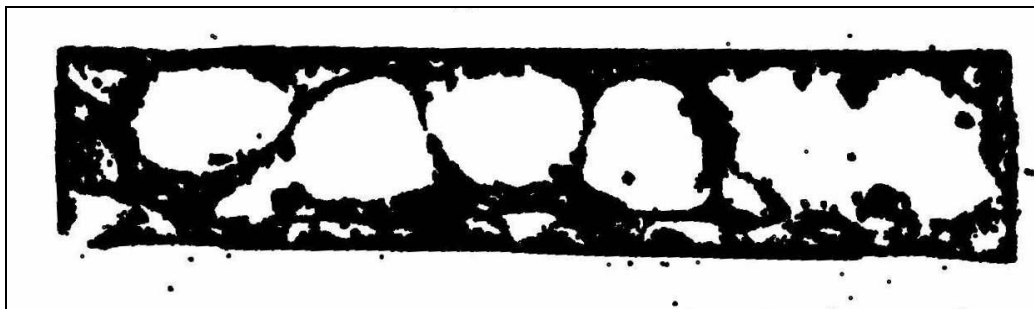**Figure 20.** Scanned image of a foam sample.

Figure 21. The same image of figure 21, ready to be analyzed after a sequence of filters and actions.

A grid with a detection of 15 pixel^2 was used to obtain all the data about the cells geometry; with the exception of the area and the orientation, all the other average parameters values (sphericity, convexity, aspect ratio and diameter maximum) were weighted average values, where the weight was the area of the cell itself.

To measure the mean volume-weighted star volume (Eq. 3) and the surface density (Eq. 6) the distance between the chord spacing was set as 20 pixels, to obtain a chords' number of about 200 per time, and each image was rotated four times of 90 º each.

3.3.2. Compression test

Compression tests were performed on squared (Fig. 22) pieces of foam of 30mm x 30mm to avoid the edge effect and the single cell's influence on the test.
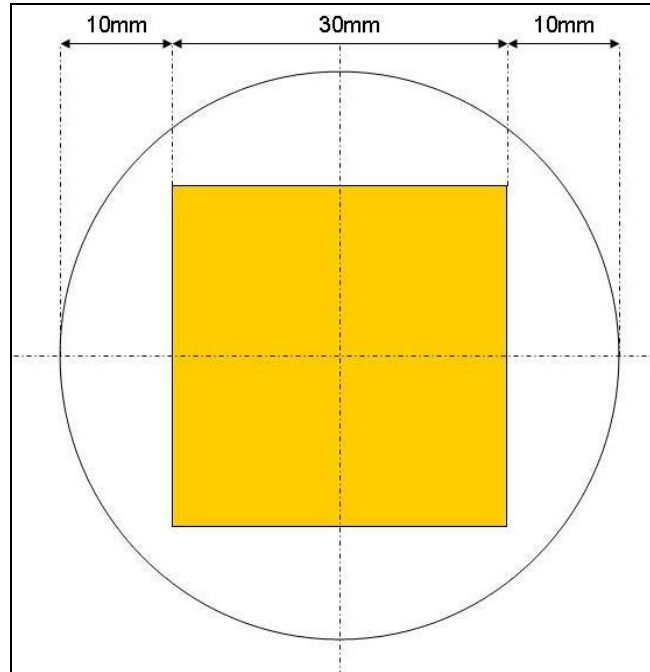

Figure 22. Compressive test's sample.

Prior testing, the foam was stored at 50% RH at a temperature of 23 ºC for at least 48 hours. Tests were performed at room temperature.

Foam was compressed in a Zwick Z2.5 (Zwick GmbH & Co. KG, Ulm, Germany), equipped with a 2 kN load cell KAP-Z (A.S.T. Angewandte System Technik GmbH, Dresten, Germany), with a compressive speed that corresponds to 10% of sample height per minute. The chosen speed was 1 mm/min. Maximum force was set to 2000 N.

Young's modulus was calculated as the slope of the initial compressive stress increase at low strain up to the first stress peak.

Three tests per semple were run.

3.3.3. Confocal Laser Scanning Microscopy

A confocal laser scanning microscopy, besides offering observation of thin optical section of thick, intact specimens, has several advantages: gives a high resolution, the wavelength can be chosen more precisely and can be used to take three dimensional images.

The microstructures of the two different kinds of foam were analyzed with confocal laser scanning microscopy (CLSM), using conventional fluorescence dyeing.

Distilled water was stained with Acridin Orange (0.2% mixture) and added, in the same amount as usual, according to the recipes, to the other ingredients. Both the mixing and the baking process were performed as usual. After 24 hours at 50% RH and 23 ℃ CLSM studies were performed. The CLSM used was LEICA TCS SP2 (Heidelberg, Germany) and two different kinds of objectives were utilized: 5x 0.12 NA and 10x 0.3 NA. Where NA is the numerical aperture and is a measure of how much of the re-emitted fluorescence light is collected by the objective.

3.4. Oscillatory measurements

All oscillatory measurements were performed in Stresstech rheometer (Rheologica Instruments, Lund, Sweden) using a parallel plate system with an upper plate of 30 mm in diameter. Samples were placed on a bottom plate whose temperature was controlled and set at 20 °C, by an elevated temperature cell (ETC). The upper plate was lowered to 0.1 mm above the final gap to allow the trimming of the sample with a cutter. The exposed edges of the sample were greased with paraffin oil to reduce the loss of water from the sample during measurements.

A final gap of 2.2 mm was used for all measurements in the rheometers. Doughs were prepared according to the two different recipes described above.

3.4.1. Stress sweep

Stress sweeps were conducted at 1Hz to establish the linear viscoelastic region of the two different recipes. The stress sweep was performed as described above with the exception of the temperature that was set at 40 °C (after the upper plate reached the final gap the ETC rose the temperature until that value), and measured between 1 and $-1 \cdot 10^{-3}$ MPa.

Only one repetition per recipe was done and the stress corresponding to the LVE region detected and used in further oscillatory measurements.

3.4.2. Frequency sweep

Frequency sweeps at constant strain were performed once for both recipes at 40 °C (ETC rose the temperature from 20 °C to the set one). A frequency range of $1 \cdot 10^{-1}$ - $1 \cdot 10^{1}$ Hz was chosen for the measurements, performed from low to high frequency.

The constant strain was chosen in order to investigate the doughs in their LVE:

- The 40% zein dough with a strain of $2 \cdot 10^{-4}$.
- The 60% zein dough with a strain of $3 \cdot 10^{-4}$;

The mechanical spectrum was plotted and determination of the power-law parameters was done using the Cox-Merz rule (Eq. 32-33).

3.4.3. *Glass transition temperature*

Oscillatory measurements at constant strain ($3 \cdot 10^{-4}$ and $2 \cdot 10^{-4}$, for 60% zein dough and 40% respectively) and constant frequency (1 Hz) with a temperature profile were conducted to establish the glass transition temperature.

This test was performed in 60 minutes with a temperature profile established from 0 to 50 °C, three times per recipe. (Thus, after reaching the final gap, the ETC lowered the temperature from the preset value of 20 °C to the initial temperature profile value).

The glass transition temperature was determined from the maximum peak of the phase angle.

3.5. **Hyperbolic contraction flow**

Hyperbolic contraction flow was performed on the two different recipes, using an Instron Universal Materials Testing Machine model 5542 (Canton, USA). The extensional strain rates, and shear contribution were calculated using the calculated power-law parameters from frequency sweep measurements.

The nozzle had an inlet radius (r_0) of 10 mm, an outlet radius (r_1) of 3 mm, and a height (H) of 15 mm. The equivalent height, H_{eq}, was calculated to be 3.57 mm (Eq. 45).

The test was performed at 40 °C using a water bath to control the feeding cylinder's temperature at four different rates: 0.1, 0.5, 1 and 2 s^{-1} in a randomized order. This meant that Extensional rates were a little different from recipe to recipe (Tab. 2) due to the different shear thinning index n.

Extensional rate	0,1 s^{-1}	0,5 s^{-1}	1 s^{-1}	2 s^{-1}
Extensional rate 40% zein	0,10 s^{-1}	0,53 s^{-1}	1,06 s^{-1}	2,13 s^{-1}
Extensional rate 60% zein	0,11 s^{-1}	0,56 s^{-1}	1,13 s^{-1}	2,27 s^{-1}

Table 2. Different rates used in hyperbolic contraction flow measurements.

The dough was prepared according to its recipe as usual; after mixing, was rolled in a cylinder, inserted in the feeding cylinder, preheated at 40 ºC, and squeezed until reaching the outlet radius. The sample was kept at rest until the stress registered reached approximately the 0 value, than the test was performed.

The time of each test was monitored by choosing an appropriate anvil height. Each test was performed until a plateau value for the stress was reached from which the extensional viscosity was calculated and corrected for shear. The anvil height was always allowed to be larger than the equivalent height, H_{eq}, meaning that at least one nozzle volume had been squeezed through the nozzle before a plateau value was reached. The strain hardening index was estimated from the slope of each stress versus time curve (plotted in a log scale).

Each recipe was tested three times.

4. RESULTS AND DISCUSSION

4.1. Foam density model

To develop the model, thirty runs, consisting in 6 centre points, 8 axial points and 16 corner points (Tab. 3), were inserted as inputs in the program.

RUN	ZEIN [%]	PLASTICIZER [g]	FOAMING AGENT [g]	MOULD TEMPERATURE [ºC]	DENSITY [Kg/dm3]
1 cp	60	0.5	0	120	**0.314**
2 cc	50	0.75	0.3	160	**0.275**
3 cp	60	0.5	0.6	200	**0.243**
4 cc	40	0.5	0	120	**0.394**
5 cp	60	1	0	200	**0.279**
6 cp	60	1	0	120	**0.29**
7 cc	50	0.75	0.3	160	**0.297**
8 cp	40	1	0.6	200	**0.341**
9 cp	40	0.5	0.6	200	**0.368**
10 cp	40	1	0	120	**0.413**
11 cp	60	1	0.6	200	**0.251**
12 cc	50	0.75	0.3	160	**0.287**
13 cp	40	0.5	0	200	**0.419**
14 cp	40	1	0	200	**0.433**
15 cp	40	1	0.6	120	**0.26**
16 cp	60	1	0.6	120	**0.307**
17 cp	40	0.5	0.6	120	**0.324**
18 cp	60	0.5	0.6	120	**0.252**
19 cc	50	0.75	0.3	160	**0.279**
20 cp	60	0.5	0	200	**0.297**
21 cc	50	0.75	0.3	160	**0.276**
22 fc	60	0.75	0.3	160	**0.235**
23 fc	50	0.5	0.3	160	**0.289**
24 fc	50	0.75	0.3	200	**0.303**
25 fc	40	0.75	0.3	160	**0.324**

26 fc	50	1	0.3	160	**0.286**
27 fc	50	0.75	0.6	160	**0.299**
28 fc	50	0.75	0	160	**0.339**
29 cc	50	0.75	0.3	160	**0.297**
30 fc	50	0.75	0.3	120	**0.292**

Table 3. Experiment runs: cp: corner point, cc: centre point, fc: face centred.

The program ran the ANOVA (Tab. 4) and this new structure and gave the following results:

Source	Sum of Squares	df	Mean Square	F Value	p-value Prob > F	
Model	0.071	6	0.012	40.59	< 0.0001	**Significant**
A-percentage zein	0.036	1	0.036	124.47	< 0.0001	
C-foaming agent	0.016	1	0.016	54.16	< 0.0001	
D-temperature	0.00043	1	0.000	1.48	0.2367	
AC	0.00357	1	0.004	12.25	0.0019	
AD	0.00432	1	0.004	14.84	0.0008	
C^2	0.011	1	0.011	36.31	< 0.0001	
Residual	0.007	23	0.0002914			
Lack of Fit	0.006	18	0.0003527	5.00	0.0417	Significant
Pure Error	0.000	5	0.0000706		**R-Squared**	**0.91**
Cor Total	0.078	29			**Adj R-Squared**	**0.89**

Table 4. ANOVA. A=percentage of zein, B=amount of plasticizer, C= amount of foaming agent, D= temperature and the other terms, such us AC, means their product, such as the multiplication between factor A and C, and so on.

The Model F-value of 40.59 implies the model was significant, there's only a 0.01% chance that a "Model F-Value" this large could occur due to noise. Moreover values of "Prob > F" less than 0.5% indicated model terms were significant; thus A (percentage of zein), C (amount of foaming agent), D (temperature) and the other factors AC, AD and C^2 are significant.

Only the p-value of temperature indicated that temperature was not significant by itself, but since hierarchy is a condition *sine qua non*, and since the factors AD was significant the temperature was significant as well.

In addition the R-Squared value of 0.91 and the Adjusted R-Squared value of 0.89 showed that the model fitted the reality quite well.

The only bad aspect was the "Lack of fit F-value" of 5.00 which implied that was significant meaning that a further investigation among the residuals was necessary to accept the model as true.

The "Normal Probability Plot" (Fig. 24) indicates whether the residuals follow a normal distribution, in which case the point will follow a straight line; while the "Externally Studentized Residuals" (Fig. 25) indicates how many standard deviations the actual value deviates from the value predicted referring to this measure as an "externally studentized residual".

These plots led to think of the presence of outliers; in particular the second plot showed a point (run number 10 in the randomized order developed by the program) out of the studentized limits.

The number of replication used, 1 instead of 3 or more as the good practice would have suggested, and the previous consideration made think the model was satisfactory.
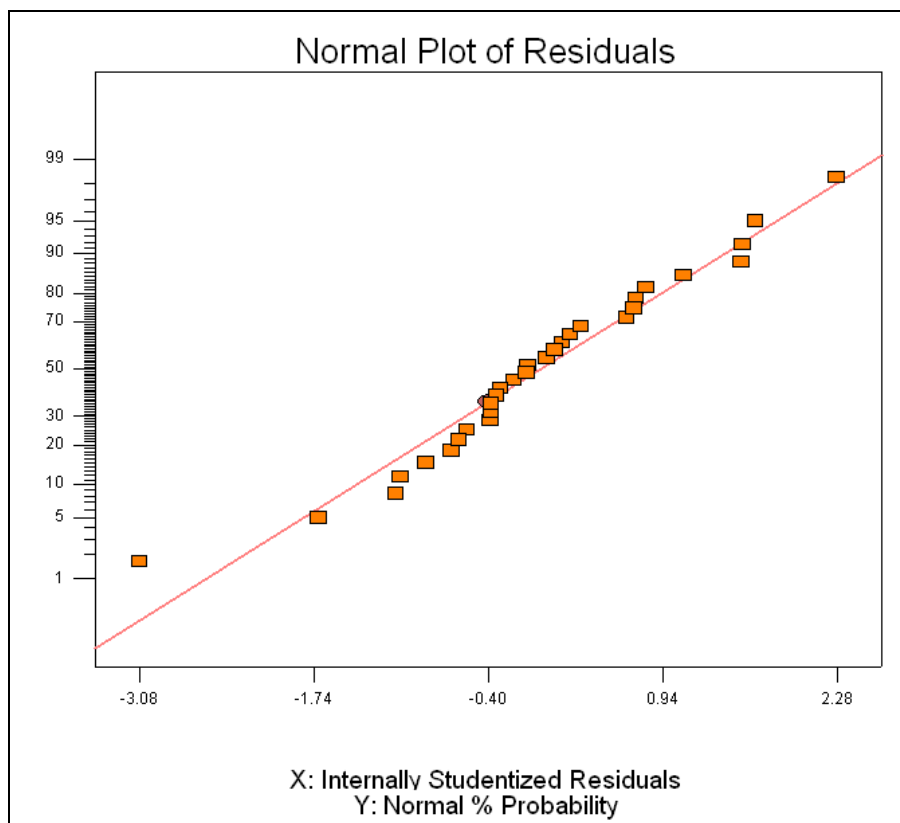
Figure 24. Normal Probability Plot.
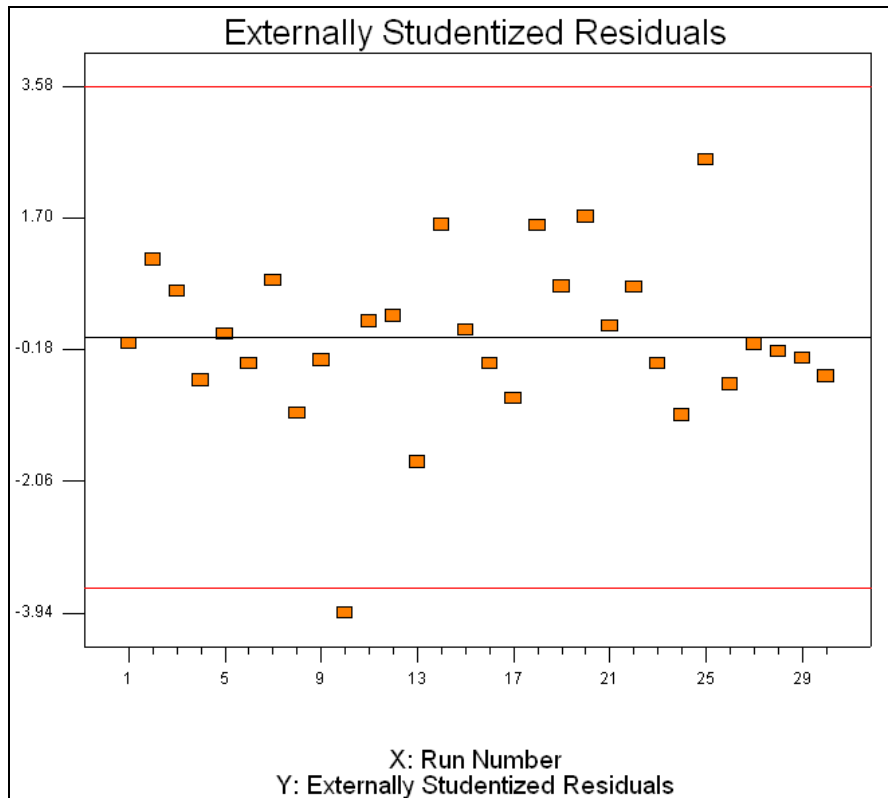
Figure 25. Externally Studentized Residuals Plot.

Due to the ANOVA the following equations were found:

Final Equation in Terms of Coded Factors:

Density   =
+0.285167
  -0.04489   * A
  -0.02961   * C
+0.004889   * D
+0.014938   * A * C
  -0.01644   * A * D
+0.038333   * C^2

Final Equation in Terms of Actual Factors:

Density   =
+0.303938
+0.000592   * percentage zein-starch
  -0.60322   * foaming agent

+0.002177   * temperature

+0.004979   * percentage zein-starch * foaming agent

-4.1E-05   * percentage zein-starch * temperature

+0.425926   * foaming agent^2

The last developing the model valid was its validation. Three different trials (Tab. 5) were made for each recipe: 53.75% of zein, 0.5g of plasticizer, 0.6g of foaming agent and 170 ºC as mould temperature.

According to the model's point prediction, the confidence interval at 95% was [0.27 Kg/dm^3; 0.30 Kg/dm^3], and since density resulted belonging to this interval (Tab. 5) the model was taken as valid.

RUN	ZEIN [%]	PLASTICIZER [g]	FOAMING AGENT [g]	MOULD TEMPERATURE [ºC]	DENSITY [Kg/dm^3]
1	53.750	0.500	0.600	170	**0.285**
2	53.750	0.500	0.600	170	**0.273**
3	53.750	0.500	0.600	170	**0.276**

Table 5. Validation runs.

Thanks to Design Expert, some 3D surfaces representing the relations among factors, AD and AC, in terms of density were pictured. In these pictures, on the floor, the curves are plotted with a constant density, that anyway are expressed in better way by other plots (Fig. 26-30)
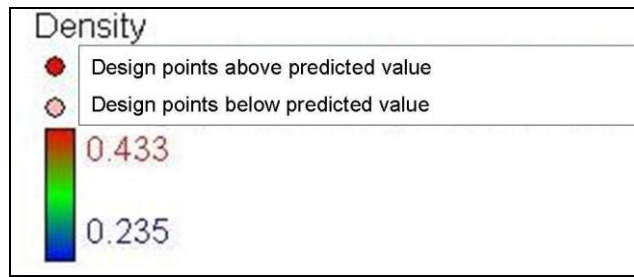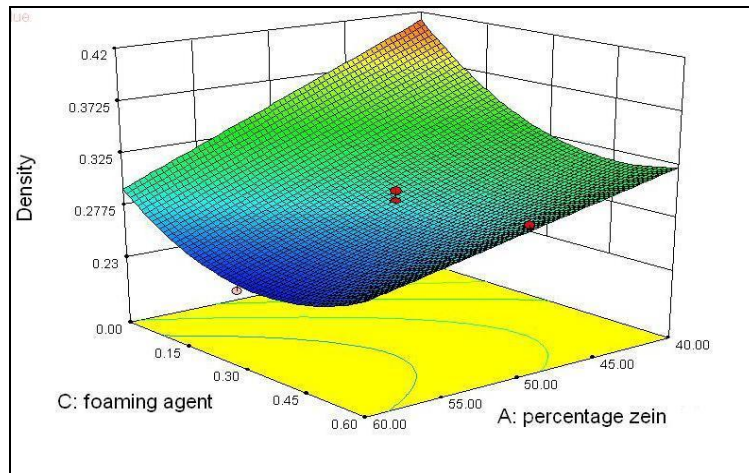
Figure 26. Legend for the following plots.

Figure 27. 3D surface representing the interaction between foaming agent and of zein.
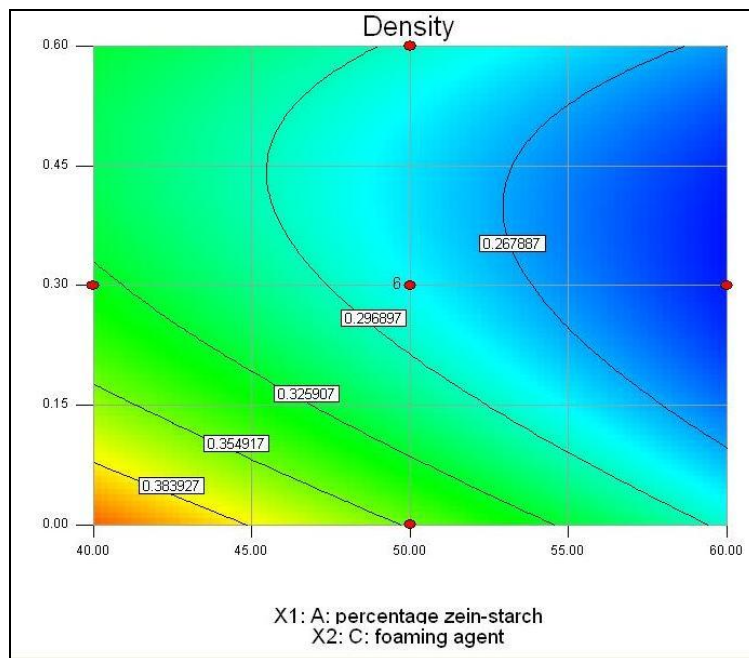

Figure 28. 2D surface representing the interaction between foaming agent and zein amount. The curves are constant density curves and the points in red are the measured points.
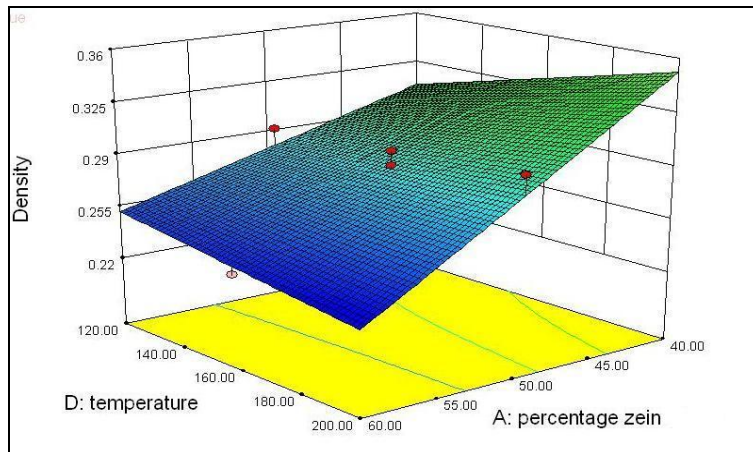
Figure 29. 3D surface representing the interaction between temperature and amount of zein.
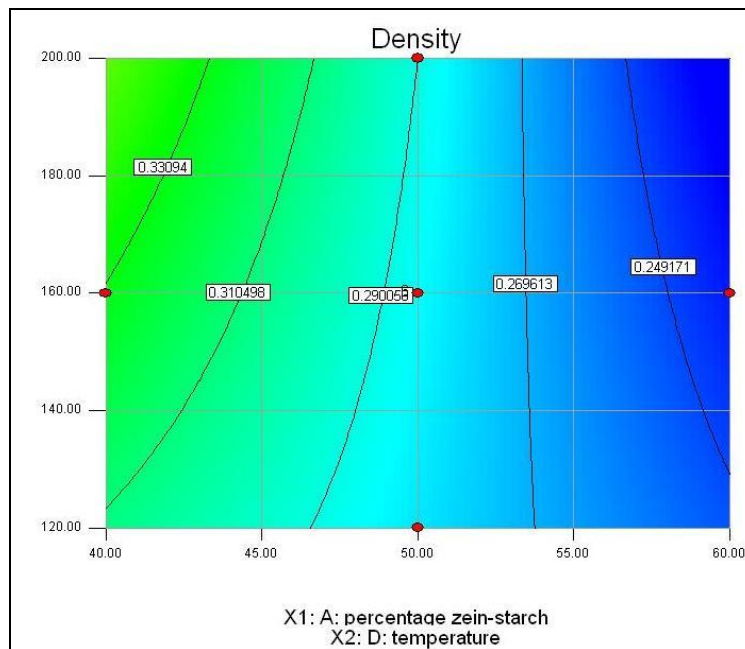

Figure 30. 2D surface representing the interaction between temperature and zein amount. The curves are constant density curves and the points in red are the measured points.

Since the density can be considered directly connected to the size and the number of foam bubbles, the model allowed to make some considerations about the foaming process.

The main factors involved were the amount of zein and foaming agent, while plasticizer has no influence even if is necessary to form dough; in particular the more zein and foaming agent the lower value of density.

The interaction terms and the quadratic one explain the complexity of the process.

Terms AC an C^2 illustrate the connection among foaming agent and percentage of zein in density terms; with a constant value of zein, higher density has a parabolic behavior meaning that the

negative density peak is reached with a medium amount of foaming agent, as can be seen in the previous pictures.

The term AD could be interpreted as the relationship between the recipe and the foaming process: in dough with high amount of zein temperature makes the density lower, while has the opposite effect with dough characterized by a high amount of starch.

In conclusion, this process is rather complex and the causes might be identified in the presence of water that act like a foaming agent during its evaporation, the swelling speed of the starch is related to the oven temperature and to dough properties such as strain hardening.

According to the model, two main recipes, giving same density but different foam structure, were found.

The first one was: 40% zein, 0.5g of plasticizer, 0.6g of foaming agent, 6.5 g of distilled water and 120 ºC was the mould temperature.

The second one was: 60% zein, 0.5g of plasticizer, 0g of foaming agent, 6.5 g of distilled water and 120 ºC was the mould temperature.

The eight runs made, four per recipe, confirmed the model's prediction (Tab. 6).

RUN	ZEIN [%]	PLASTICIZER [g]	FOAMING AGENT [g]	MOULD TEMPERATURE [ºC]	DENSITY [Kg/dm^3]
1	40.0	0.5	0.6	120.0	**0.305**
2	40.0	0.5	0.6	120.0	**0.332**
3	40.0	0.5	0.6	120.0	**0.334**
4	40.0	0.5	0.6	120.0	**0.325**
RUN	ZEIN [%]	PLASTICIZER [g]	FOAMING AGENT [g]	MOULD TEMPERATURE [ºC]	DENSITY [Kg/dm^3]
1	60.0	0.5	0.0	120.0	**0.331**
2	60.0	0.5	0.0	120.0	**0.317**
3	60.0	0.5	0.0	120.0	**0.328**
4	60.0	0.5	0.0	120.0	**0.315**

Table 6. Recipes' validation runs.

According to the values above, the interval for the density were ($p=0.05$):

- 40% zein foam: 0.324 ± 0.021 [Kg/dm^3]
- 60% zein foam: 0.323 ± 0.012 [Kg/dm^3]

4.2.   Foam characterization

The two recipes mentioned in the previous paragraph led to two foams characterized by the same density but quite distinct cells structures. The following analyses were performed, on those two different final products, to elucidate the ingredients' influence on the cells geometry, which obviously is related to mechanical properties.

4.2.1.   Image analysis

Results from Image AnalySIS are presented in the table below (Tab. 7).

	Area	Area Max	Aspect Ratio	Inner diameter Max	Orientation	Sphericity	Convexity
40% zein	0.55±0.14	33.60±29.77	2.12±0.41	0.66±0.05	41.02±3.25	0.29±0.06	0.71±0.05
60% zein	3.55±0.67	71.85±26.23	2.39±0.74	1.81±0.24	9.94±2.29	0.22±0.09	0.72±0.01

Table 7. Cells characterization measurements (p=0.05).

Both recipes showed similar cell structures demonstrated the aspect ratio, sphericity and convexity.

The main difference was represented by the area of the single cell; the 40% zein foam had 0.55 mm^2 whereas the 60% zein had a value at least 6 times bigger. It's obvious that such a big cell, closed into the frame, was not free to expand, which is also shown by the orientation value. In fact, the inertia moment of the cloud of points representing the cell, formed an angle of 8° with the main axis of the foam's sample, which means that the gas bubble grew more in the horizontal direction than the vertical since it was compressed by the two hot plates.

Results from stereology (Tab. 8) led to the conclusion that foam characterized by 40% zein had cells with isotropic shape while the 60% zein foam did not.

	Volume weighted star volume	Surface density
40% zein	1.89±1.32	3.36±0.48
60% zein	29.46±14.35	1.57±0.07

Table 8. Data deriving from Stereologycal analysis (p=0.05).

This was confirmed by the quite low value the surface density of the 60% zein foam: a cell with such a big value of volume weighted star volume would have had a higher value of surface density if would have been isotropic.

All these considerations confirmed once more the model proposed in the previous paragraph; assuming equal the weighs of the two different polymers, is obvious that, to obtain a similar density value, with such a different cell structures, the number of cells, first, and their shape, second, should be different.

The CLSM micrographs confirmed this, at least in what referred to number of cells. As can be seen in the pictures the differences between the thicknesses of the lamellas of the two recipes are clear.
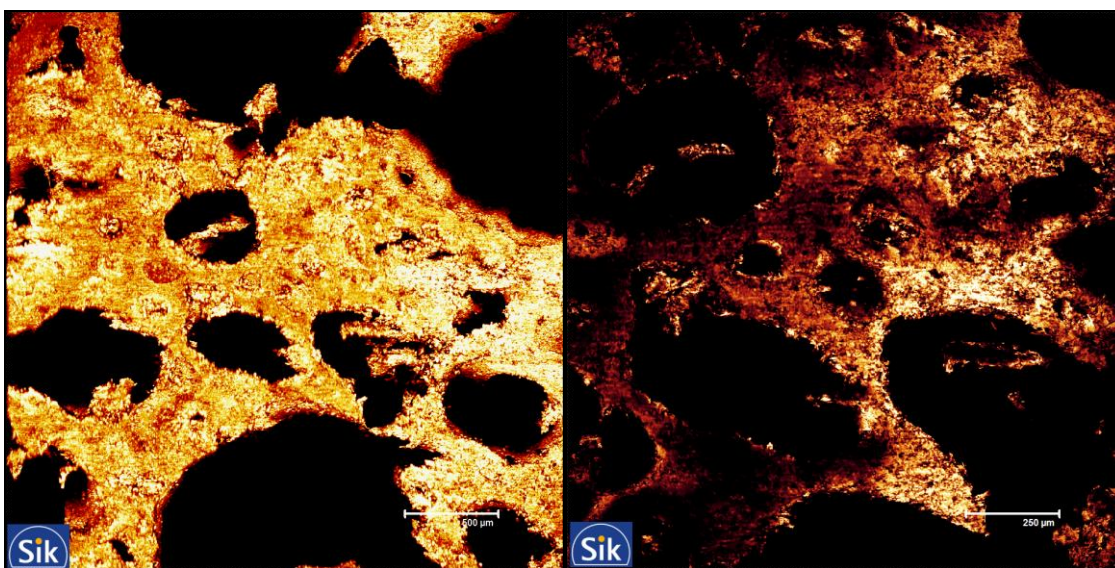
Figure 30. Pictures of 40% zein foam, the one on the left with a magnification power of 5x and the other with a 10x.
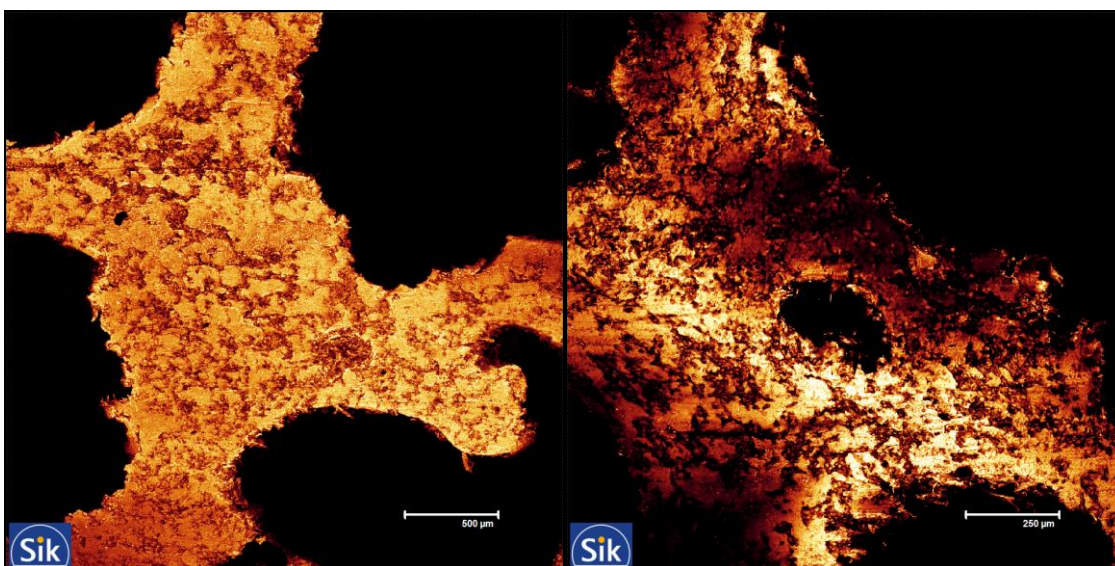
Figure 31. Pictures of 60% zein foam, the one on the left with a magnification power of 5x and the other with a 10x.

In the 40% zein (Fig. 30) with both 5x and 10x magnification power, the structure is really porous.

Instead the 60% zein (Fig. 31) has a more compact structure where the lamellas do not have any point of weakness, even when observed with the higher magnification.

Nevertheless, should be remembered that 40% zein was characterized by the presence of foaming agent that could be considered the cause of the porous structure.

Thus, it is reasonable concluding that the foams had equal density since cell size, number and shape were different. Moreover, even the lamellas had different structure according to the presence of foaming agent.

4.2.2. Compressive test

Compressive test were performed on the two foams having equal density and the Young's was determined (Tab. 9).

RECIPE	Young's modulus average value	Standard deviation
40% zein foam	6.67	0.80
60% zein foam	14.29	2.48

Table 9. Data from compressive tests, average and standard deviation values.

These values and the development of the stress-strain curve of the tests showed that the 60% zein foam had a more hard and brittle structure than the 40% zein foam.

In particular, the 40% zein compression test plot (Fig. 32) didn't have the characteristic three regions but these could be considered melted together; cells started collapsing almost immediately when the load was increased and the structure become more and more compact until the densification zone was reached. This could be explained by the great number of cells and even their small dimension.

In Fig. 33 it's clear that 60% zein foam was more fragile and brittle, so after 10% of deformation it collapsed. From that point (when the load reached the value 0) the plot and the following test didn't make sense since this was performed on a set of foam crumb. This could be explained basically by the fact that the entire load was taken by one cell, whose collapse caused the collapse of the sample.

The amount of zein can be considered the cause of this difference, in particular the more zein the more brittle the foam.
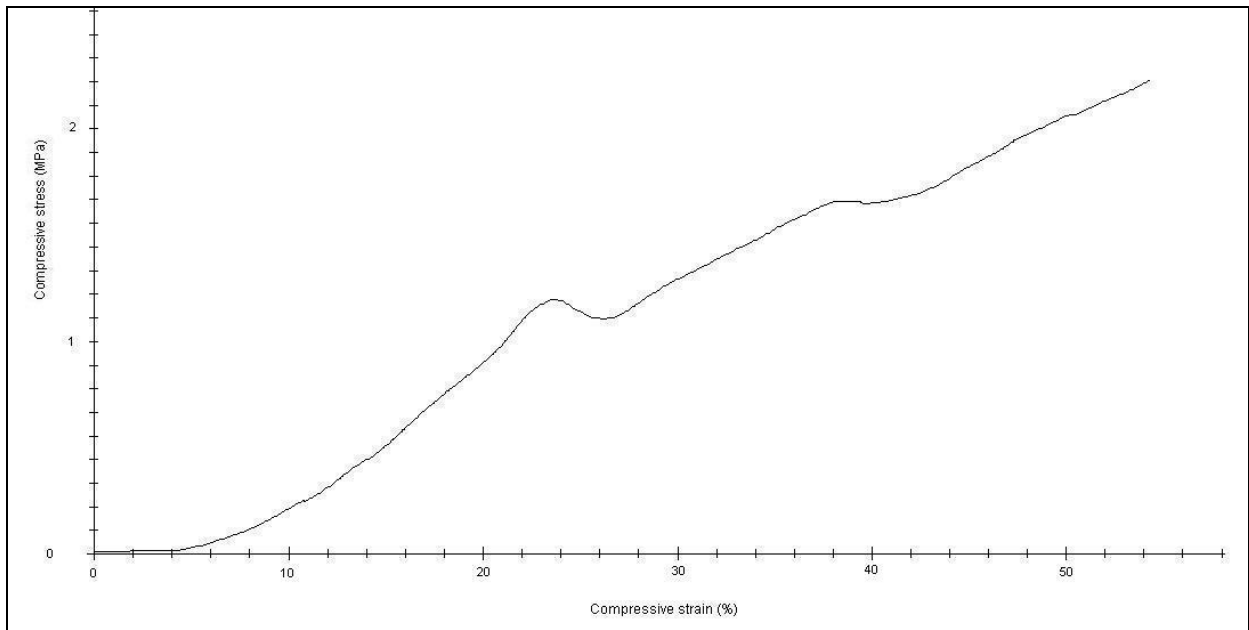
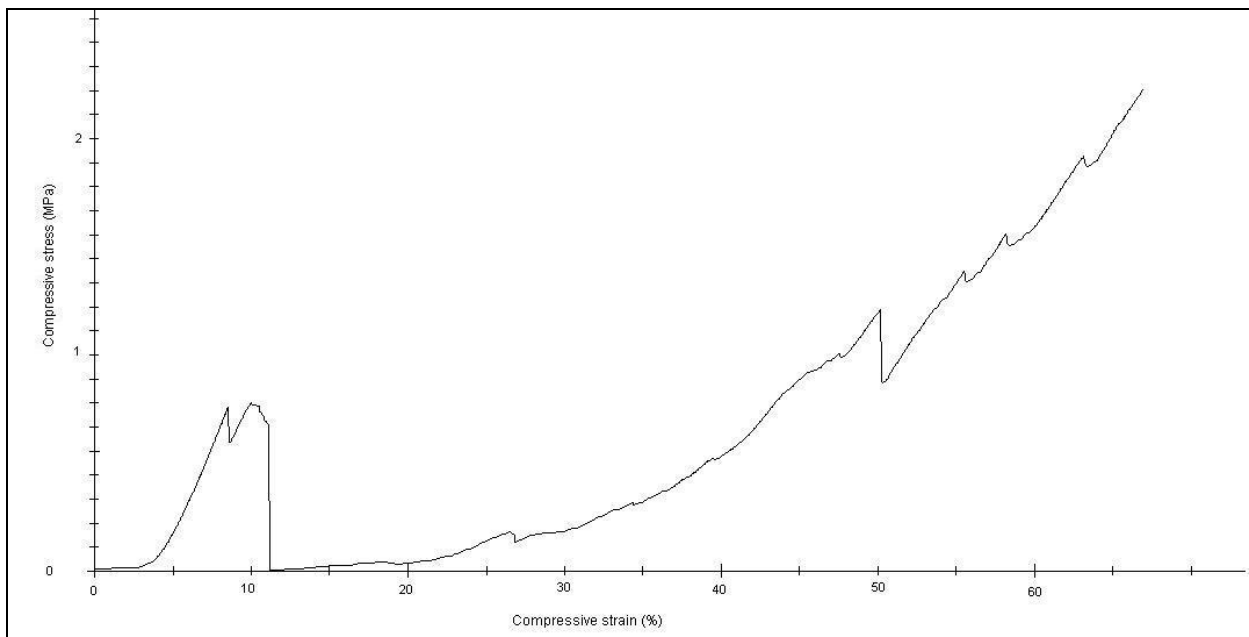**Figure 32.** Compressive test plot for 40%zein foam.

Figure 33. Compressive test plot for 60%zein foam.

4.3. Oscillatory test

Oscillatory test are used to examine and characterize viscoelastic materials. The two different doughs, resulting from the recipes identified in the previous paragraph, were the object of the analysis to understand how the ingredients influenced the dough properties and consequently the foam. In particular in this project the test was used both to identify the T_g (temperature profile)

and to characterize the doughs (frequency sweep) obtaining the consistency and power law indices necessary to run the hyperbolic contraction flow analysis.

These two oscillatory tests were performed in the LVE region, identified by a stress sweep test.

4.3.1. Stress sweep

Stress sweep tests were run to locate the LVE region of the two different doughs, which is where the Hook's, Newton's and Cox-Merz's laws are valid. In this region the G' and G'' values are constant, showing a plateau in their plots (Fig. 35). According to their curves, the strains were that identified the LVE were figured out:

- 40%zein: $2 \cdot 10^{-4}$
- 60%zein: $3 \cdot 10^{-4}$
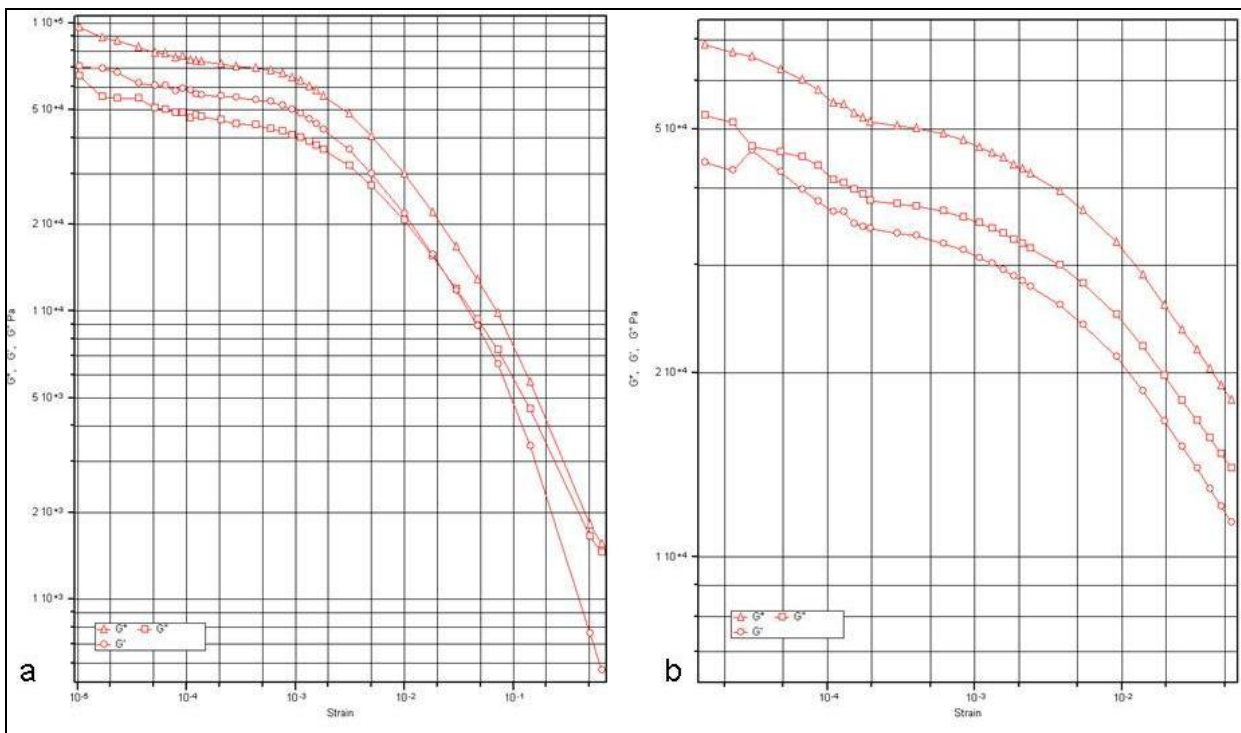
Figure 35. Stress sweep for 40%zein dough (a) and 60% zein (b). At low strain values the curves plotted do not behave like expected, but this could be related to the effect of noise and the choice of a not proper number of position resolution during the measurement

4.3.2. *Frequency sweep*

The frequency sweep tests (Fig. 36) were run to characterized the doughs; the Cox-Merz rule was applied and the consistency index and (K) and power-low index (n) were detected (Tab. 10). Both doughs were shear-thinning as expected. In particular the 40% zein dough showed a more shear-thinning behavior than the 60% zein, leading to the conclusion that the amount of starch was the responsible for this difference.

RECIPE	CONSISTENCY INDEX (K) [kPa^n]	POWER-LAW INDEX (n)
40% zein dough	23	0.41
60% zein dough	19	0.52

Table 10. Consistency index and power law index from the Cox-Merz's rule.
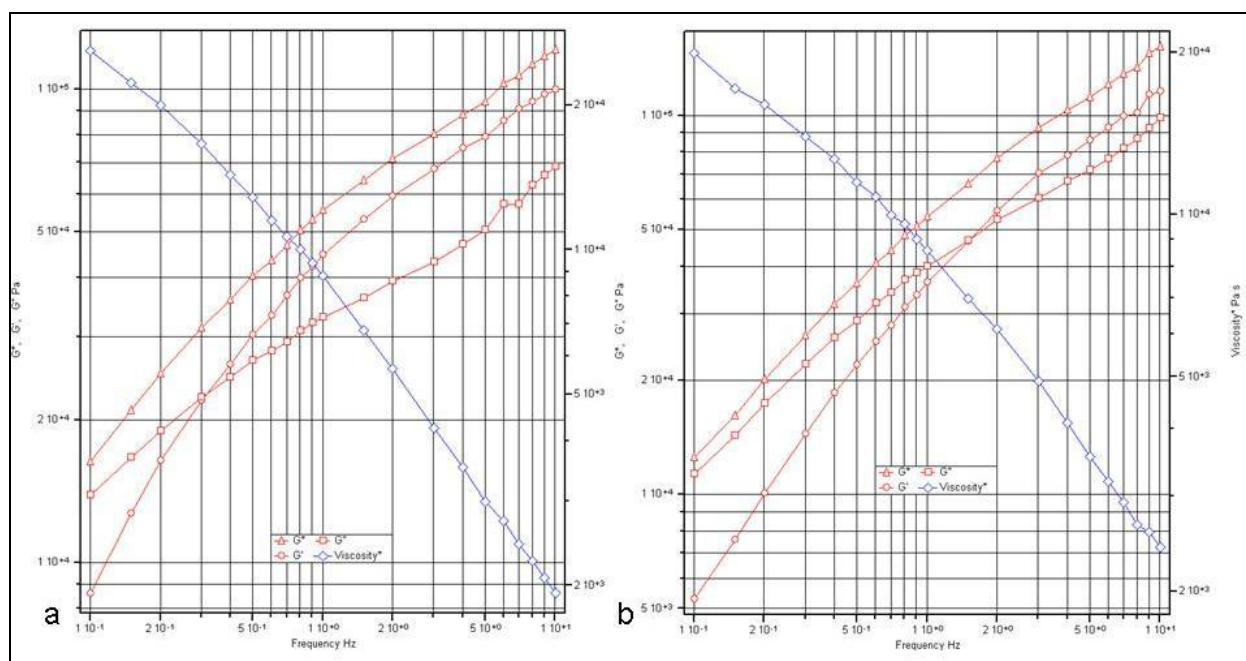
Figure 36. Frequency sweep for 40% zein dough (a) and 60% zein dough (b).

4.3.3. *Glass transition temperature*

Three different tests per recipe were run and the peaks in the phase angle curves gave the following results (Tab. 11).

	Tg (40% zein) [C°]	Tg (60% zein) [C°]
RUN 1	19.7	22.6
RUN 2	22.2	17.3
RUN 3	21.8	20.1
Interval	21 ± 3	20 ± 6

Table 11. T_g interval for both recipes (p=0.05).

There's no statistical evidence proving the difference in the T_g among the two different doughs. This could be explained considering that both samples had the same amount of plasticizer and water while the differences in terms of zein was not enough to lead to a change in the T_g.
Looking at the phase angle plots (Fig. 37) was evident that the peaks are reached almost at the same temperature but their values are difference according to the recipe, in particular 40% zein dough has a lower value, meaning that has a more elastic behavior that the 60% zein one.
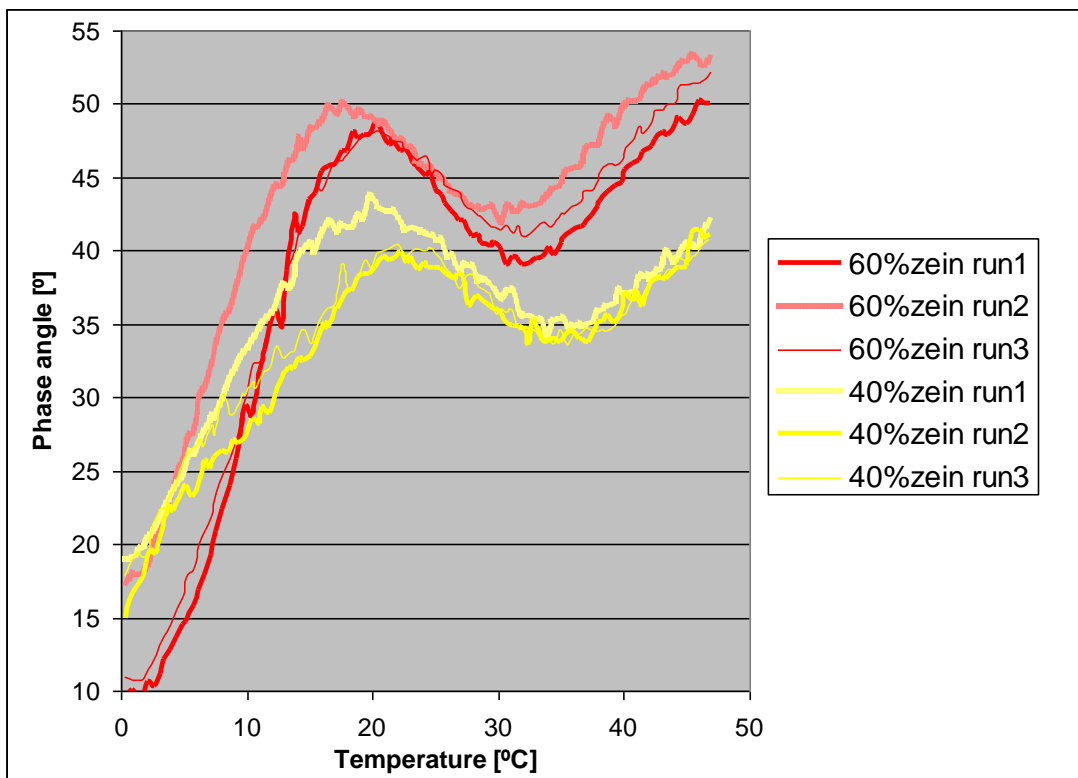

Figure 37. Phase angle curves for 40%zein and 60%zein dough.

4.4. Hyperbolic contraction flow

Hyperbolic contraction flow tests were to analyze the uniaxial extensional viscosity.

Object of the analysis were the two doughs leading to the different foams in order to figure out how their foaming properties were related to the different ingredients. Thus both recipes were tested at similar extension rates and the extensional viscosity (Fig. 38) and strain hardening index (Tab. 12) were determined.

According to the following figures both doughs showed a tension-thinning behavior and in particular the 60% zein had higher value of extensional viscosity.
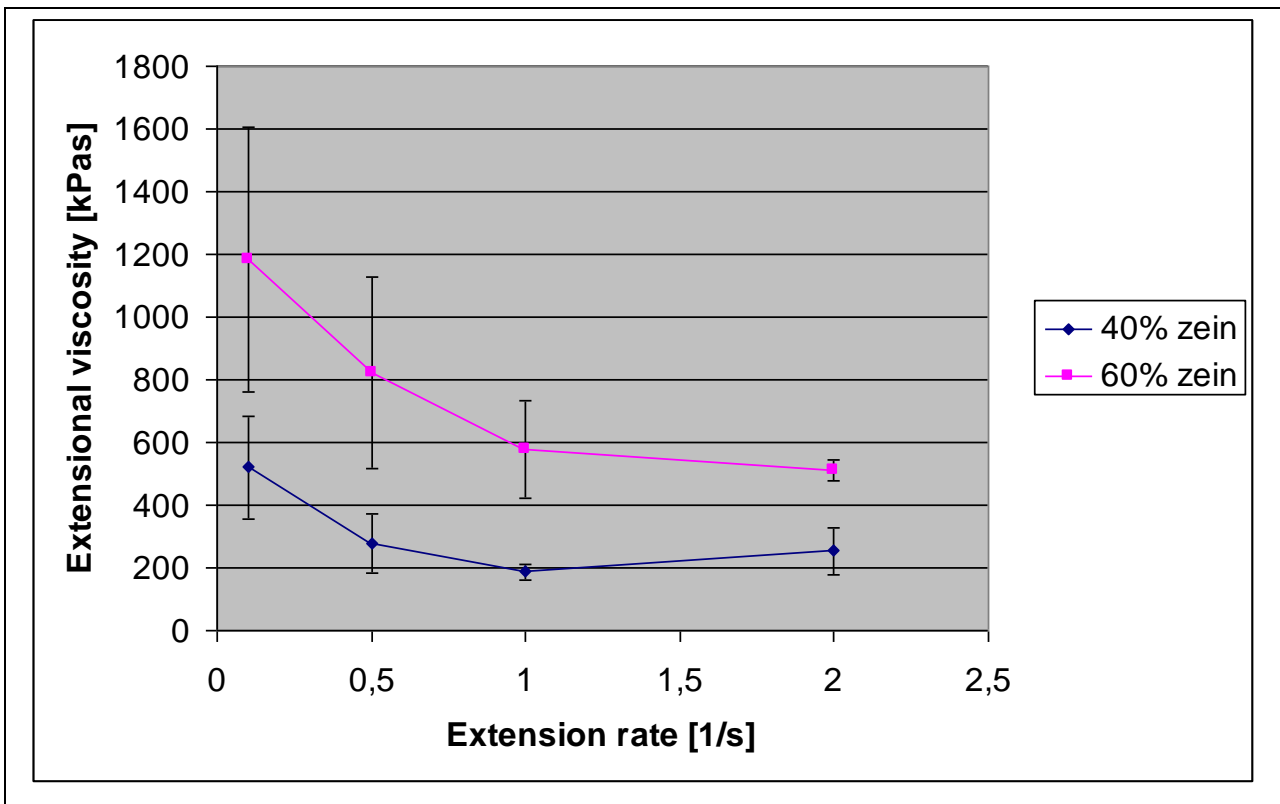
Figure 38. Extensional viscosity plotted as sample mean with standard deviation.

Tests at different strain rates were performed in randomized order, to minimize the effect of a possible ageing, but since the standard deviation detected was extremely large results should be taken with care.

In spite of that, was possible to assert that the amount of zein, in the doughs tested, is proportional to the extensional viscosity and moreover, that the content of foaming agent (at least in the percentage tested) did not affect the dough properties.

Strain hardening indices were determined as given in Tab. 12.

Extension rate	0.1 [s^{-1}]	0.5 [s^{-1}]	1 [s^{-1}]	2 [s^{-1}]
40% zein	0.98 ± 0.27	1.27 ± 0.03	1.27 ± 0.10	1.50 ± 0.34
60% zein	0.99 ± 0.30	1.42 ± 0.49	1.40 ± 0.43	1.74 ± 0.41

Table 12. Strain hardening index for both recipes at the different rates (p=0.10).

Table 12 shows that both doughs showed were strain hardening for extension rates higher than 0. s^{-1} and increasing with increasing extension rate.

It should be remembered that the strain hardening indices presented above were lower than the real ones; in fact the model used, fitted the real data in all the interval of time, while the slope of such data sometimes was even higher (Appendix 3).

The comparison between those two series of data led to say that the amount of zein is connected to the strain hardening effect, the more zein the higher strain hardening index; meaning that zein had the ability to form entanglements.

Some clarifications are necessary. First of all it is almost impossible to detect the real extension rate and the value of strain hardening index during foaming at the set temperature (120 ºC). Moreover high temperature decreases extensional viscosity; it has been showed before this relation for wheat flour dough, and could be assumed true in this case as well (Vliet T., 2008).

According to these results, the dough with a higher amount of zein had better foaming properties in terms of extensional viscosity and strain hardening at 40 ºC.

5. CONCLUSIONS AND FUTURE WORK

The fact that the foam with worse cells characteristic (isotropy and cells average area) was originated by dough with better foaming properties (extensional viscosity and strain hardening) lead to think that another cause affected the foaming process.

This could be identified with the swelling of the starch; during mixing the starch granules absorb water and inside the hot mould they start gelatinization and swelling until the foam is totally dried.

Obviously the rate of this process is related to the baking temperature; while the starch is swelling the cells have the possibility to grow.

In Fig. 25 this effect is evident, in particular for 40% zein foams: the higher the temperature, the faster the drying of the foam and the higher the density.

This phenomenon seems to have less importance for dough of 50% zein where the effect of the temperature related to amount of starch is almost not influent, while for 60% zein recipes higher mould temperature lead to a lower density.

One possible cause of this behavior could be represented by the rate of water vaporization that in this case behaves like a foaming agent.

From the previous results it is possible to state that the amount of zein influences the dough properties in terms of extensional viscosity and strain rate and the foam's structure in terms of cells' size and anisotropy. However, this last effect could be considered related to the shape of the frame used: the orientation of the cells in the foams with higher amount of zein was in fact almost the same as the final product. Moreover the higher the quantity of zein, the more brittle the foam.

The presence of foaming agent instead does not influence the dough properties, at least in the percentage analyzed, but has relevance in what is related to the density and thus the foam characteristics, according to the amount of zein.

In particular: with a low amount of zein (40%) the foaming agent has a fundamental importance in terms of porosity (the more foaming agent the more numerous the cells), while in 60% zein foams its effect is mitigated by the presence of the other foaming agent, the water.

In other words, in 40% zein dough, during the foaming process, the foaming agent has the power to create cells expanding walls, while the water vaporization does not; instead in the 60% zein their effects are summed.

The result of this sum is anyway not visible since the dough, at the foaming temperature, is not able to retain gas bubbles as well as the 40% zein dough where the swelling process of the starch is significant.

Plasticizer hasn't showed relation with density and foam structure, in the percentages investigated, but its presence is necessary to achieve a good dough.

The model proposed could be consider valid, even if could be improved with a higher number of test.

Of great interest could be making the same analysis with other frame shape, a thicker one, to obtain isotropic cells even with high amount of zein, and studying mathematical model also for cells shape and foams mechanical properties.

ACKNOWLEDGEMENTS

REFERENCES

Arendt, E.K. and Dal Bello, F. (2008) *Gluten-Free Cereal Products and Beverages*, Illustrated edn. Oxford, UK: Academic Press Inc.

Barnes, H.A. (2000) *A handbook of elementary Rheology [Electronic]*. Aberystwyth: University of Wales, Institute of Non-Newtonian Fluid Mechanics.

Dobraszczyk, B.J. and Morgenstern, M.P. (2003) Rheology and the breadmaking process. *Journal of Cereal Science*, **38**, 229-245.

Gibson L. J. and Ashby Michael F. (1997) Cellular solid, structure and properties, Cambridge university press. **5.** 176-178

Goesaert, H., Brijs, K., Veraverbeke, W.S., Courtin, C.M., Gebruers, K. and Delcour, J.A. (2005) Wheat flour constituents: How they impact bread quality, and how to impact their functionality *Trends in Food Science and Technology*, **16**, 12-30.

Lawton, J.W. (2002) Zein: A history of processing and use [Review]. *Cereal Chemistry*, **79**, 1-18.

Lawton, J.W. (1992) Viscoelasticity of Zein-Starch Doughs. *Cereal chemistry*, **69**, no4, 351-355.

Montgomery C. Douglas (2001) Design and analysis of experiments, **5-6**, John Wiley and Sons.

Mezger, T.G. (2006) *The Rheology Handbook: For users of rotational and oscillatory rheometers*, 2nd edn. Hannover: Vincentz Network.

NJ Mills (2007) Polymers foams handbook**,** Engineering and biomechanics applications and design guide. **1,5.** 2-3,88

Raymond E. Kirk, Donald F. Othmer. (1953) Encyclopedia of chemical technology. **6**, 772.

Raymond E. Kirk, Donald F. Othmer. (1953) Encyclopedia of chemical technology. **10**, 766.

Reed M. G. and Howard C.V. (1997) Surface-weighted star volume: concept and estimation, journal of microscopy, Vol. 190, 350-356

Richard F. Tester, John Karkalas, Xin Qi (2004) Starch composition, fine structure and architecture. *Journal of cereal science*, 39, 151-165.

Russ John C. and Robert T. Dehoff (2000) Practical stereology, Second edition. **1,** 1.

Schober, T.J., Bean, S.R., Boyle, D.L. and Park, S.-H. (2008) Improved viscoelastic zein–starch doughs for leavened gluten-free breads: Their rheology and microstructure. *Journal of Cereal Science*, **48**, 755-767.

Sears J.K, Darby J.R. (1982) Mechanism of plasticizer action**,** The Technology of Plasticizers, Wiley-Intersience, New York, 35-55.

Shukla, R. and Cheryan, M. (2000) Zein: the industrial protein from corn. *Industrial Crops and Products*, **13**, 171-192.

Sleeper D. Andrew (2005) Design for six sigma statistics, **10**, Kindle Edition.

Steffe, J.F. (1996) *Rheological methods in food processing engineering [Electronic]*, 2nd edn. East Lansing, MI: Freeman Press.

van Vliet, T. (2008) Strain hardening as an indicator of bread-making performance: A review with discussion *Journal of Cereal Science*, **48**, 1-9.

Weibel R. Ewald (1980) Stereological methods, Theoretical Foundations. Vol. 1, **2**, 31.

Wikström, K. and Bohlin, L. (1999a) Extensional flow studies of wheat flour dough. I. Experimental method for measurements in contraction flow geometry and application to flours varying in breadmaking performance. *Journal of Cereal Science*, **29**, 217-226.

Wikström, K. and Bohlin, L. (1999b) Extensional flow studies of wheat flour dough. II. Experimental method for measurements in constant extension rate squeezing flow and application to flours varying in breadmaking performance *Journal of Cereal Science*, **29**, 227-234.
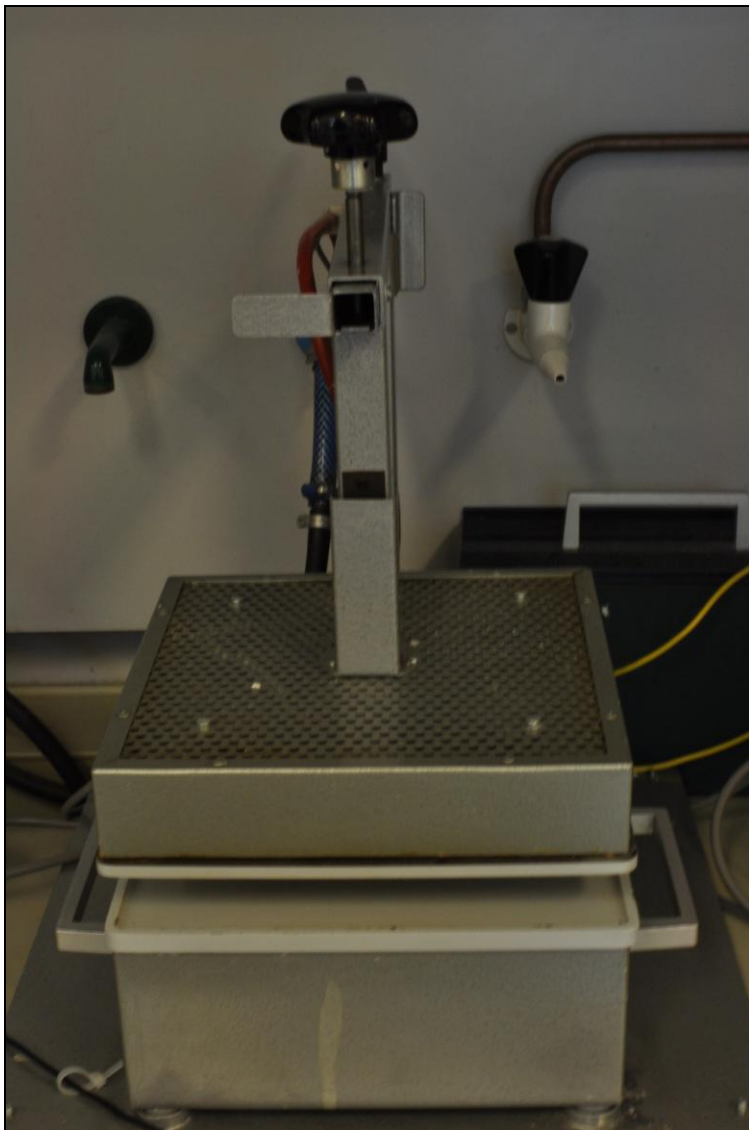
APPENDIX 1

Figure 1. The mould: it's possible to see the two plates, here placed at a distance a few centimetres.
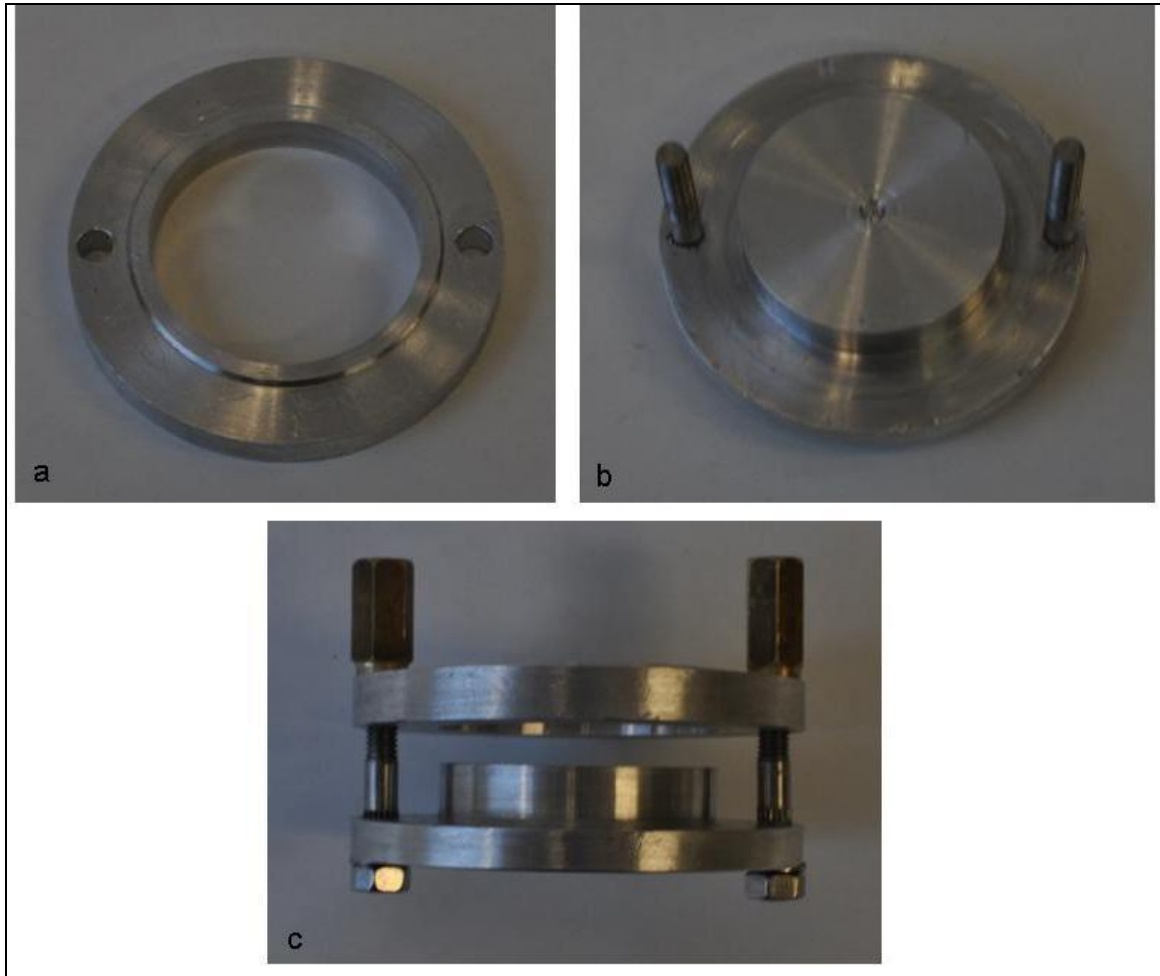
APPENDIX 2

Figure 1. The frame used. It was composed by two different parts. The properly frame (a) was filled by the dough and inserted between the hot plates, while the second part (b) was used to extract the final product without damages due to their pairing (c).
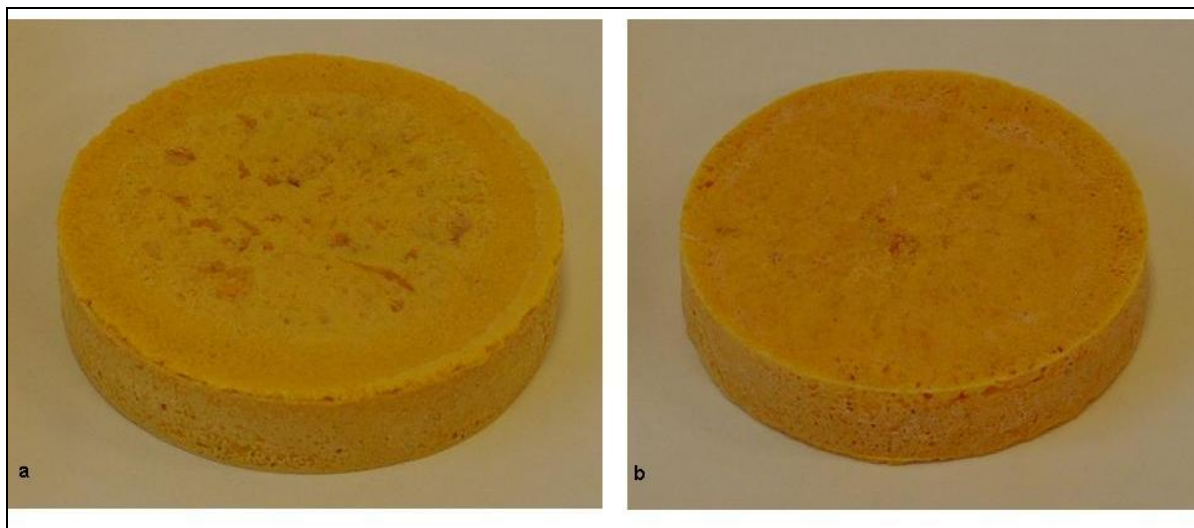

Figure 2. Foam sample, 40% zein (a) and 60% zein (b).
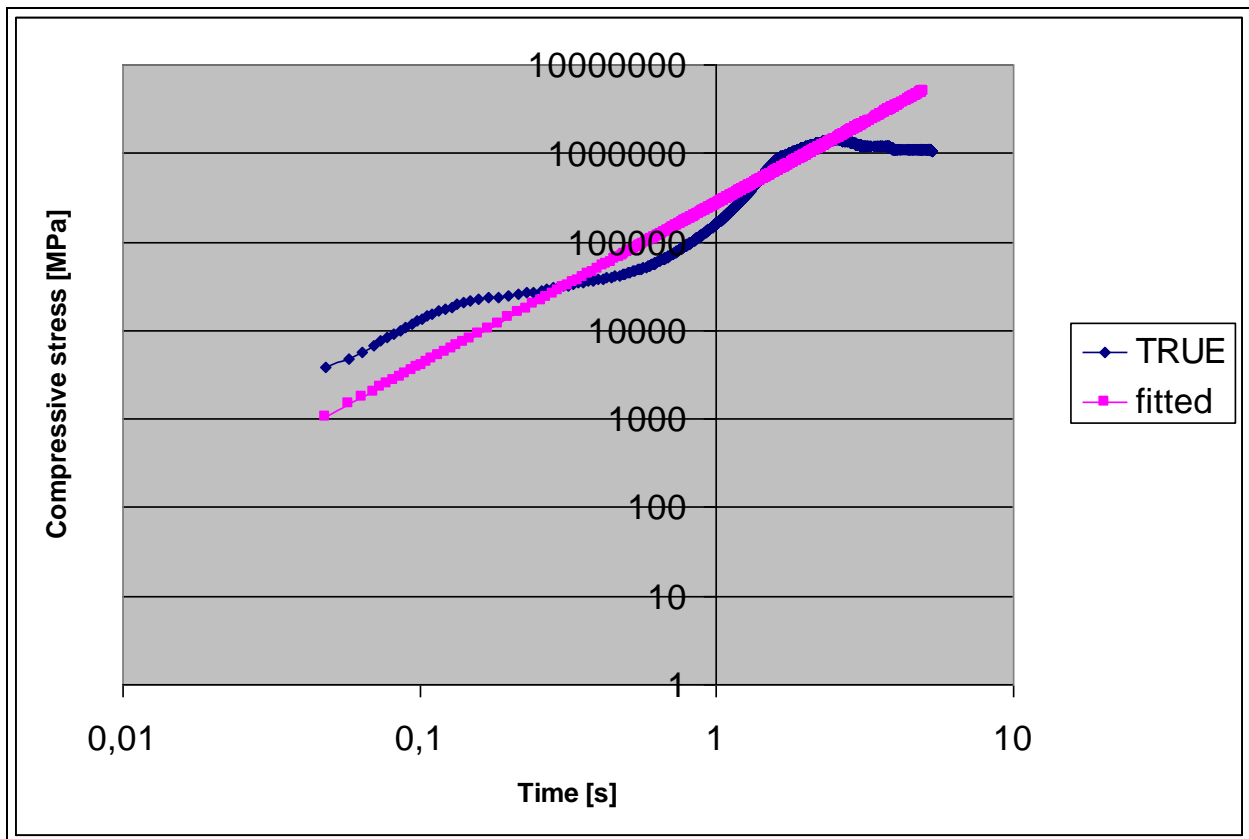
APPENDIX 3

Figure 1. Plot of the compressive stress versus time, registered during hyperbolic contraction flow, in logarithmic scale. The slope of the violet line represent the strain hardening index; it's an average value since the model used to fit the real values investigates a quite large interval of time, at least until the compressive stress is rising. Looking at the real values (blue curve), is clear how the slope is higher for time equal to 1s.